

Vertical structure

Now we will examine the vertical structure of the intense baroclinic wave using three visualization tools:

- Upper level charts at selected pressure levels
- Vertical soundings for selected radiosonde stations
- Vertical cross-sections.



Vertical structure

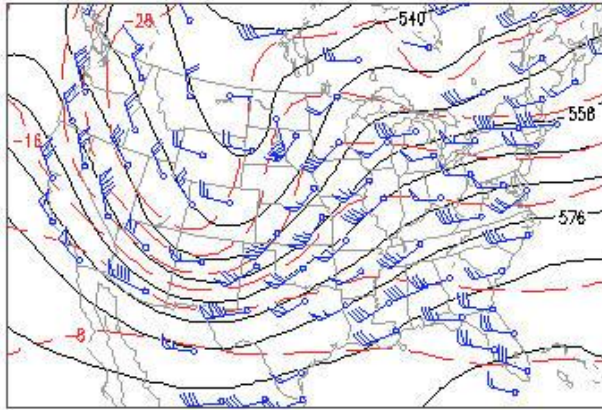
Now we will examine the vertical structure of the intense baroclinic wave using three visualization tools:

- Upper level charts at selected pressure levels
- Vertical soundings for selected radiosonde stations
- Vertical cross-sections.

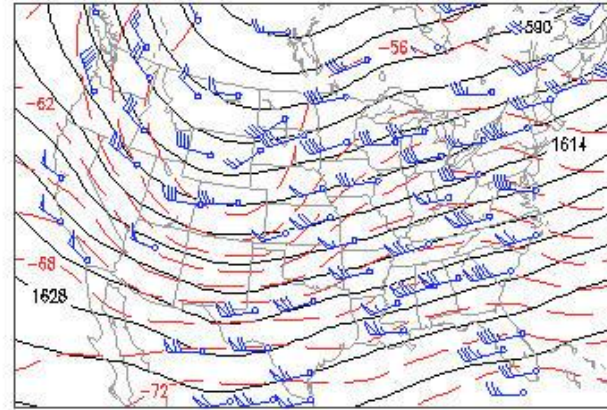


To conclude, we will review the **critical factors** involved in the development of extratropical storms.

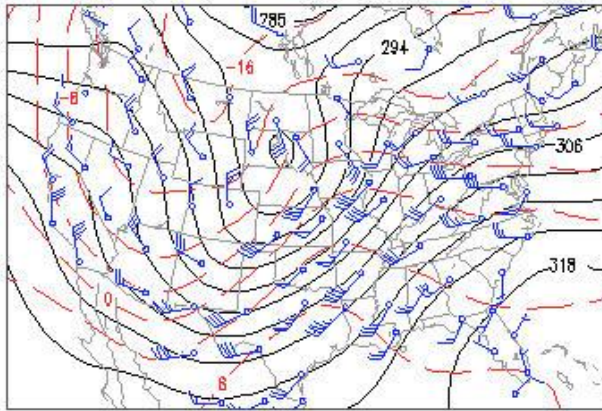
500 hPa



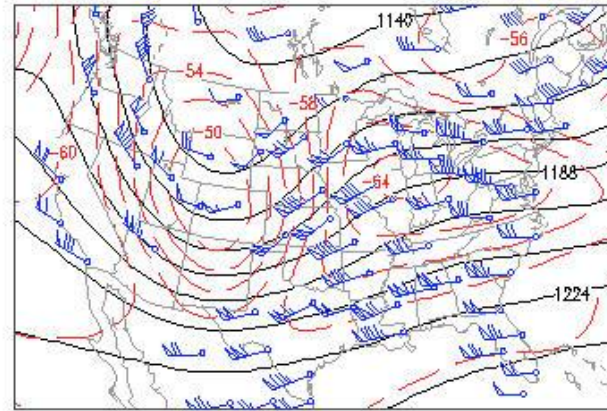
100 hPa



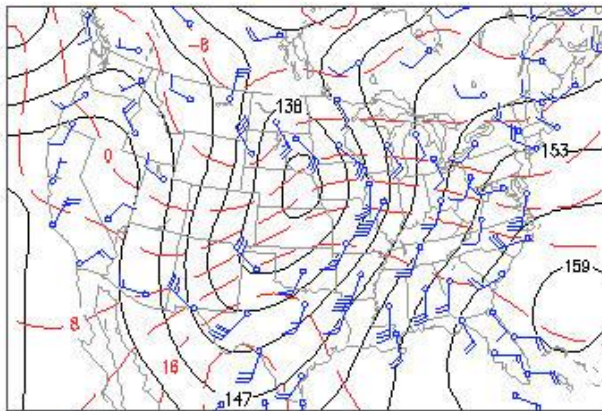
700 hPa



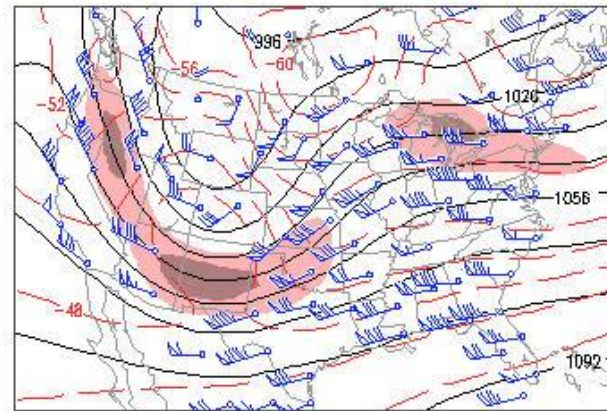
200 hPa



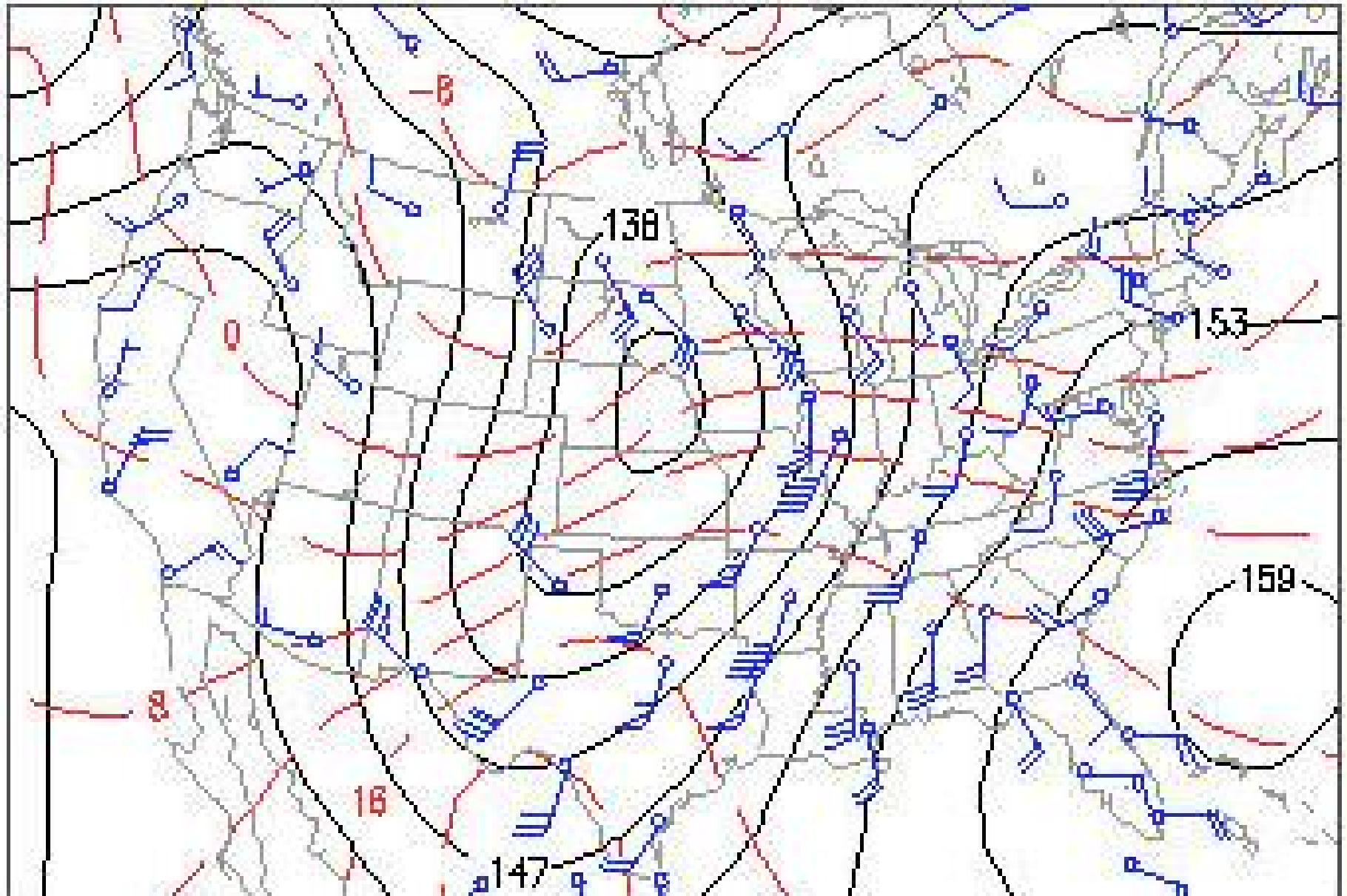
850 hPa



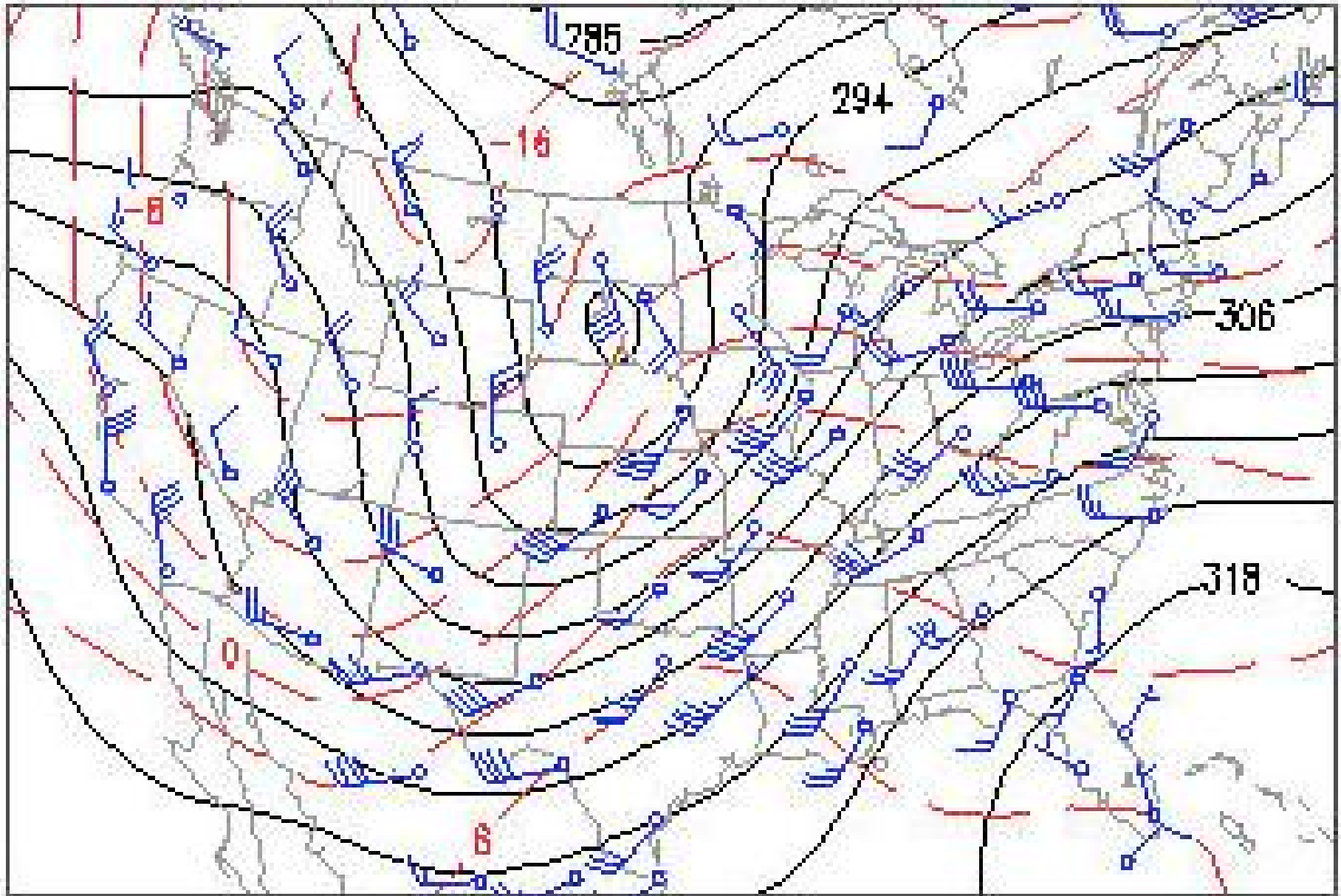
250 hPa



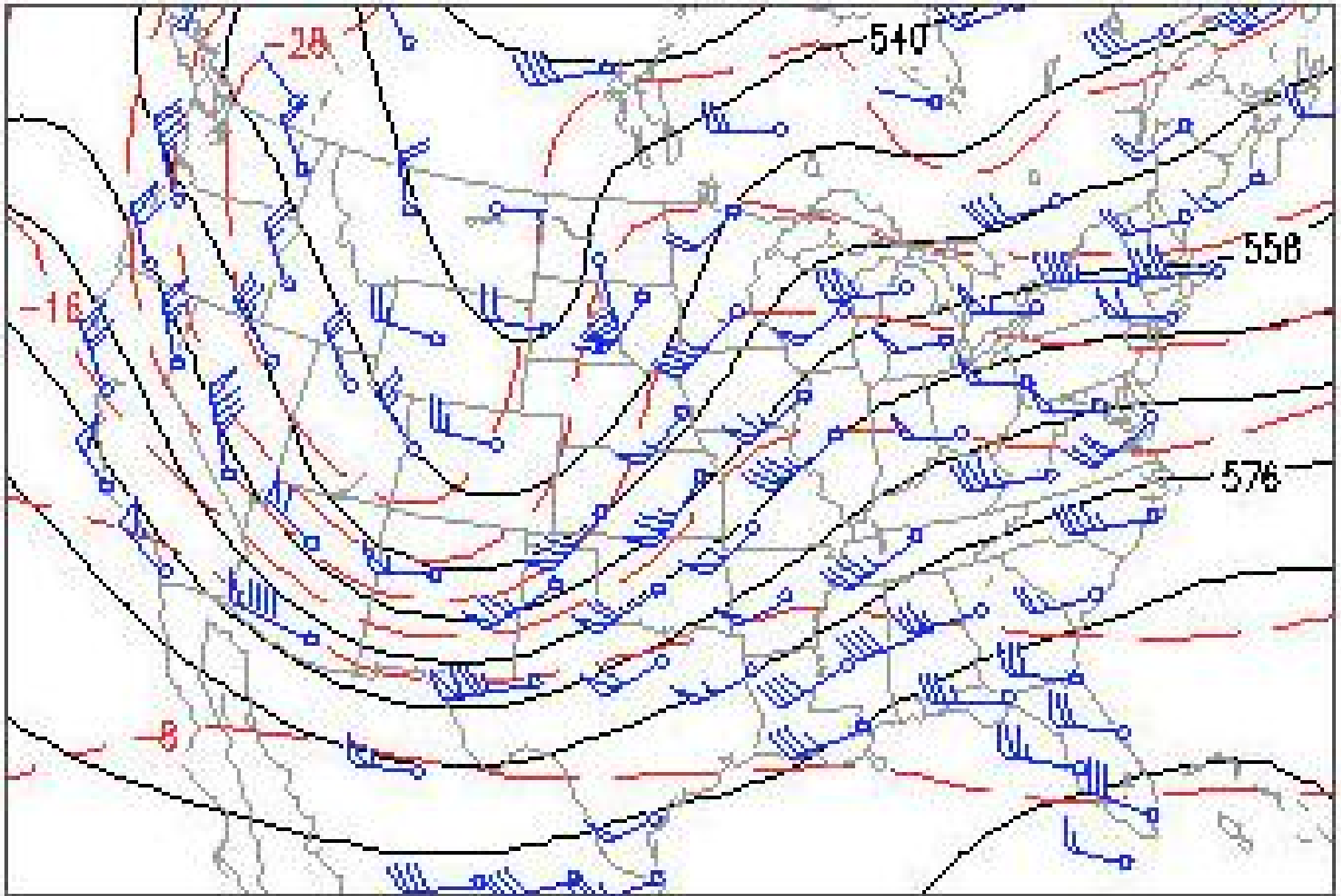
Upper level charts for 00 UTC, Nov. 10, 1998.
Geopotential height (black), temperature (red).



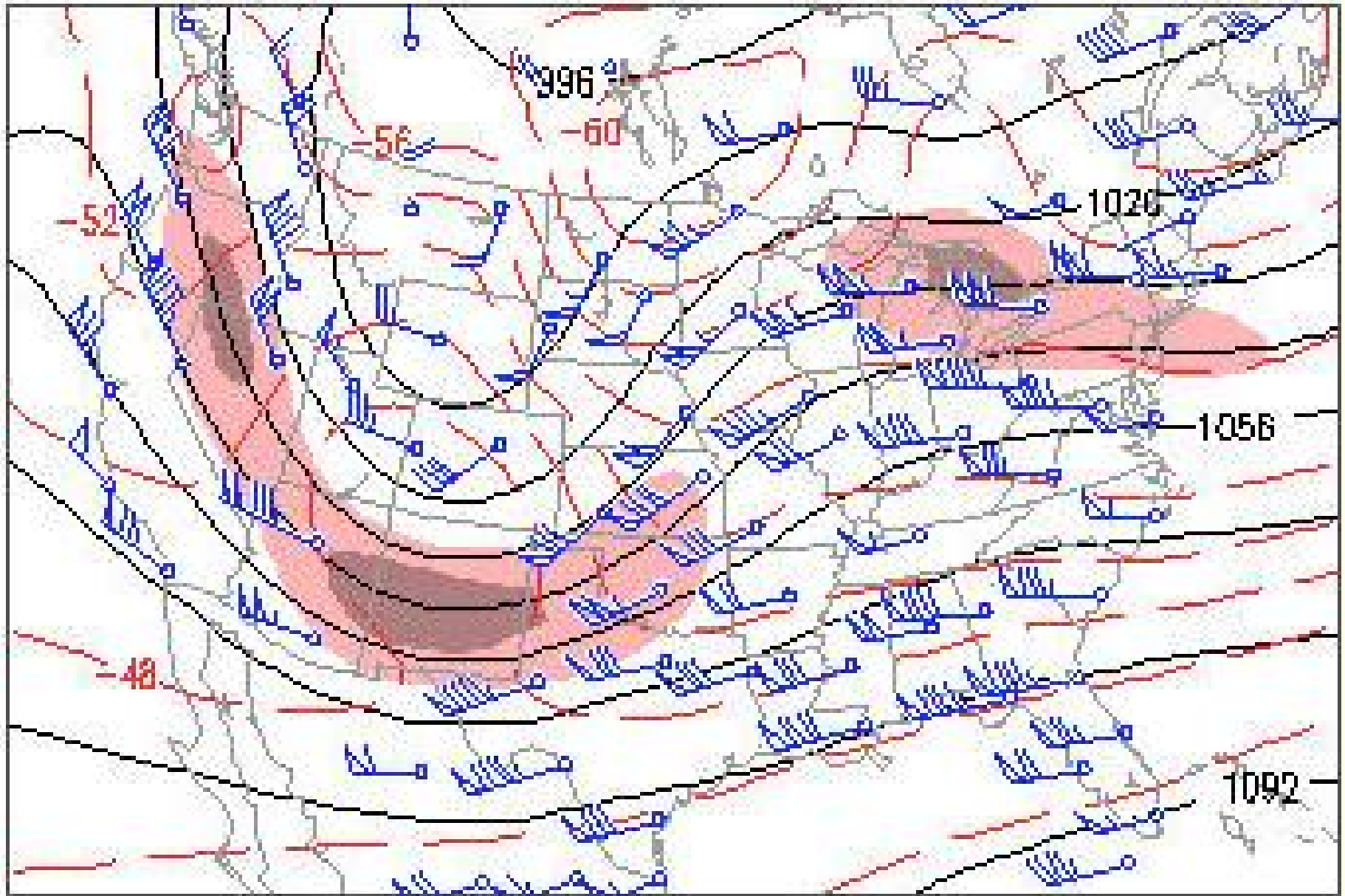
850 hPa level chart 00Z, November 10, 1998.
(contour 30 m for height, 4°C for temperature)



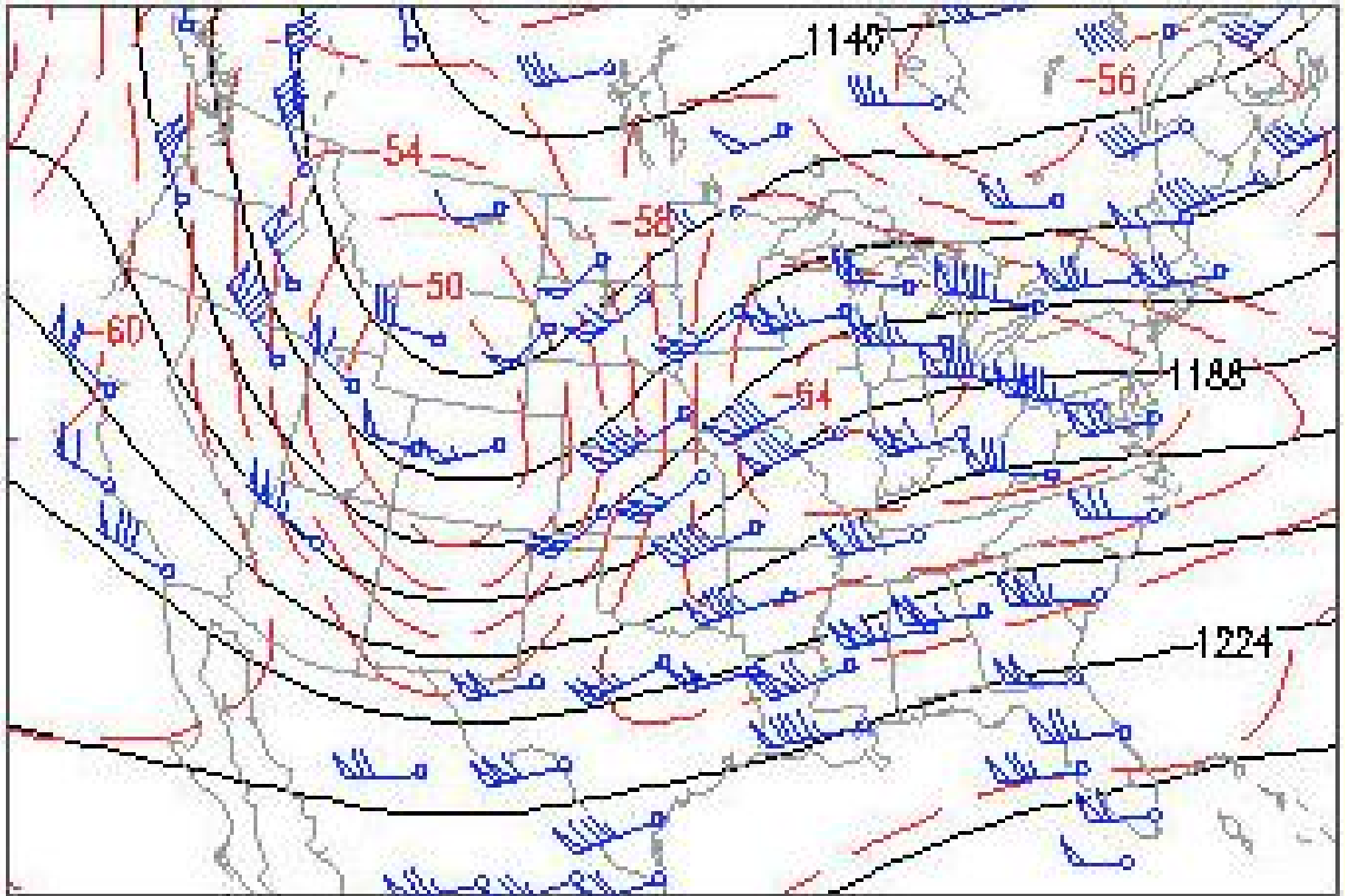
700 hPa level chart 00Z, November 10, 1998.
(contour 30 m for height, 4°C for temperature)



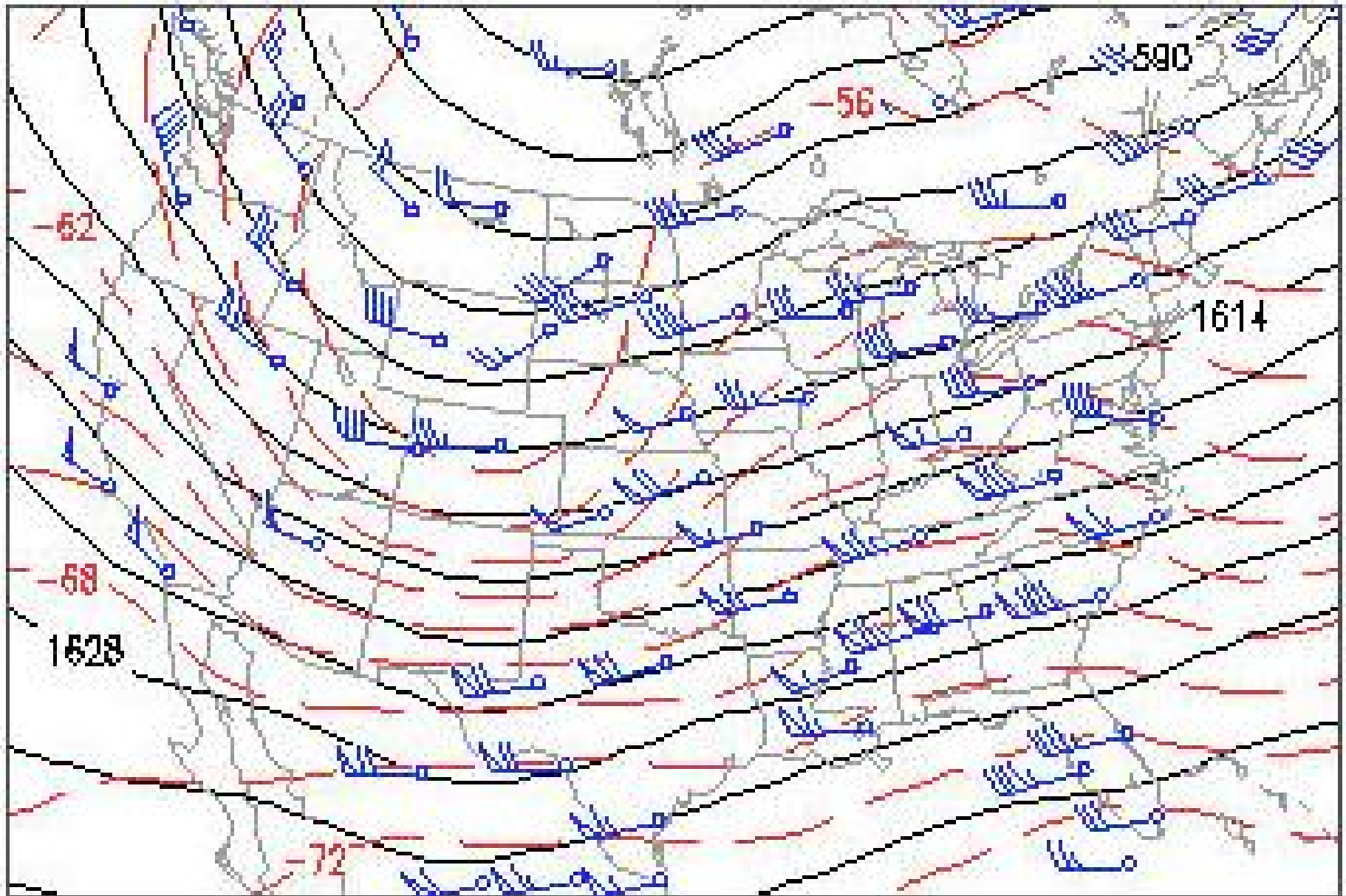
500 hPa level chart 00Z, November 10, 1998.
(contour 60 m for height, 4°C for temperature)



250 hPa level chart 00Z, November 10, 1998.
(contour 120 m for height, 2°C for temperature)



200 hPa level chart 00Z, November 10, 1998.
(contour 120 m for height, 2°C for temperature)



100 hPa level chart 00Z, November 10, 1998.
(contour 60 m for height, 2°C for temperature)

Upper Level Charts

The 850 hPa chart for 00 UTC November 10, when the associated extratropical cyclone was beginning to deepen rapidly, is examined next.

The corresponding sea level pressure and surface air temperature patterns is also shown.

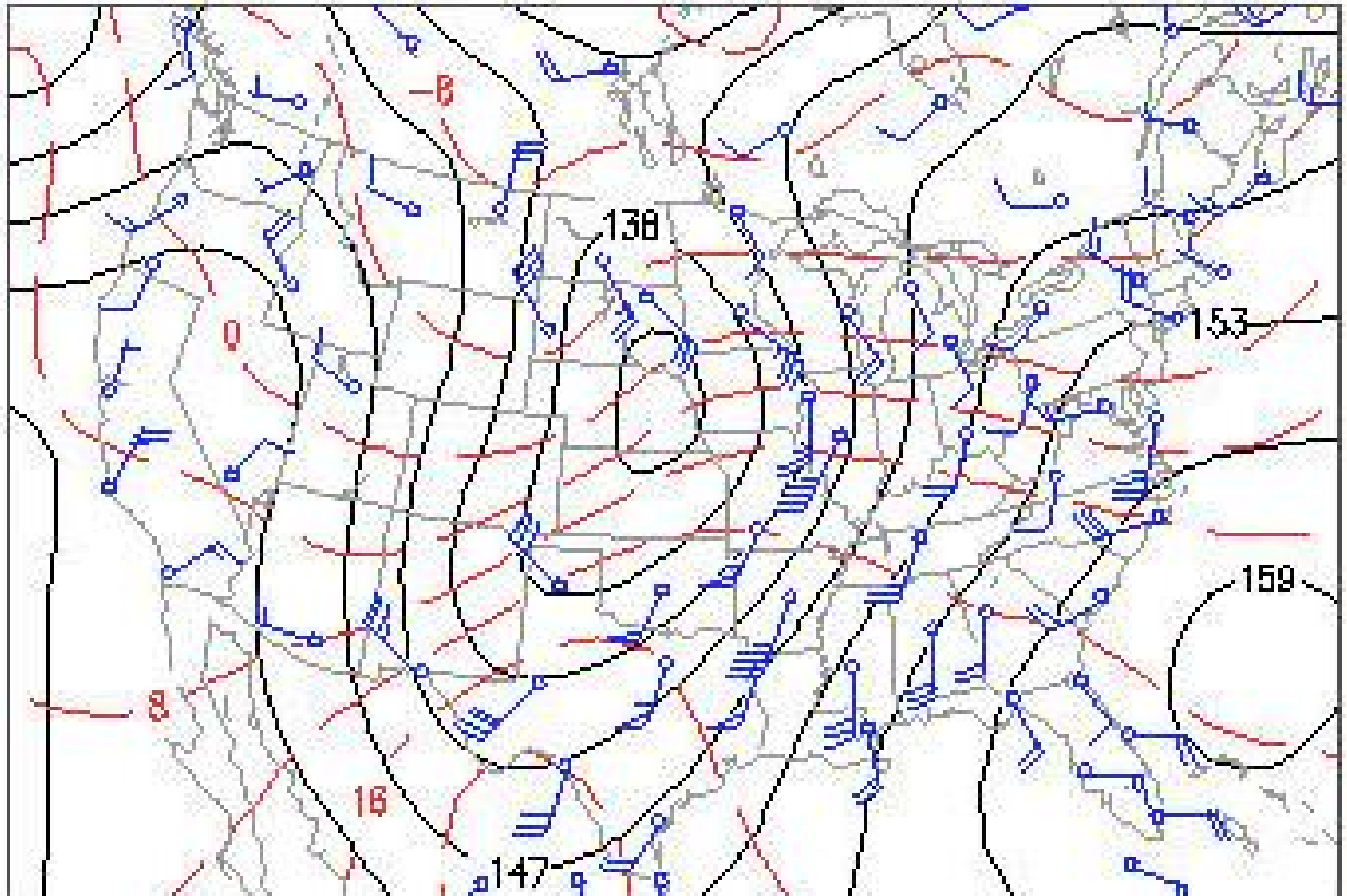
Upper Level Charts

The 850 hPa chart for 00 UTC November 10, when the associated extratropical cyclone was beginning to deepen rapidly, is examined next.

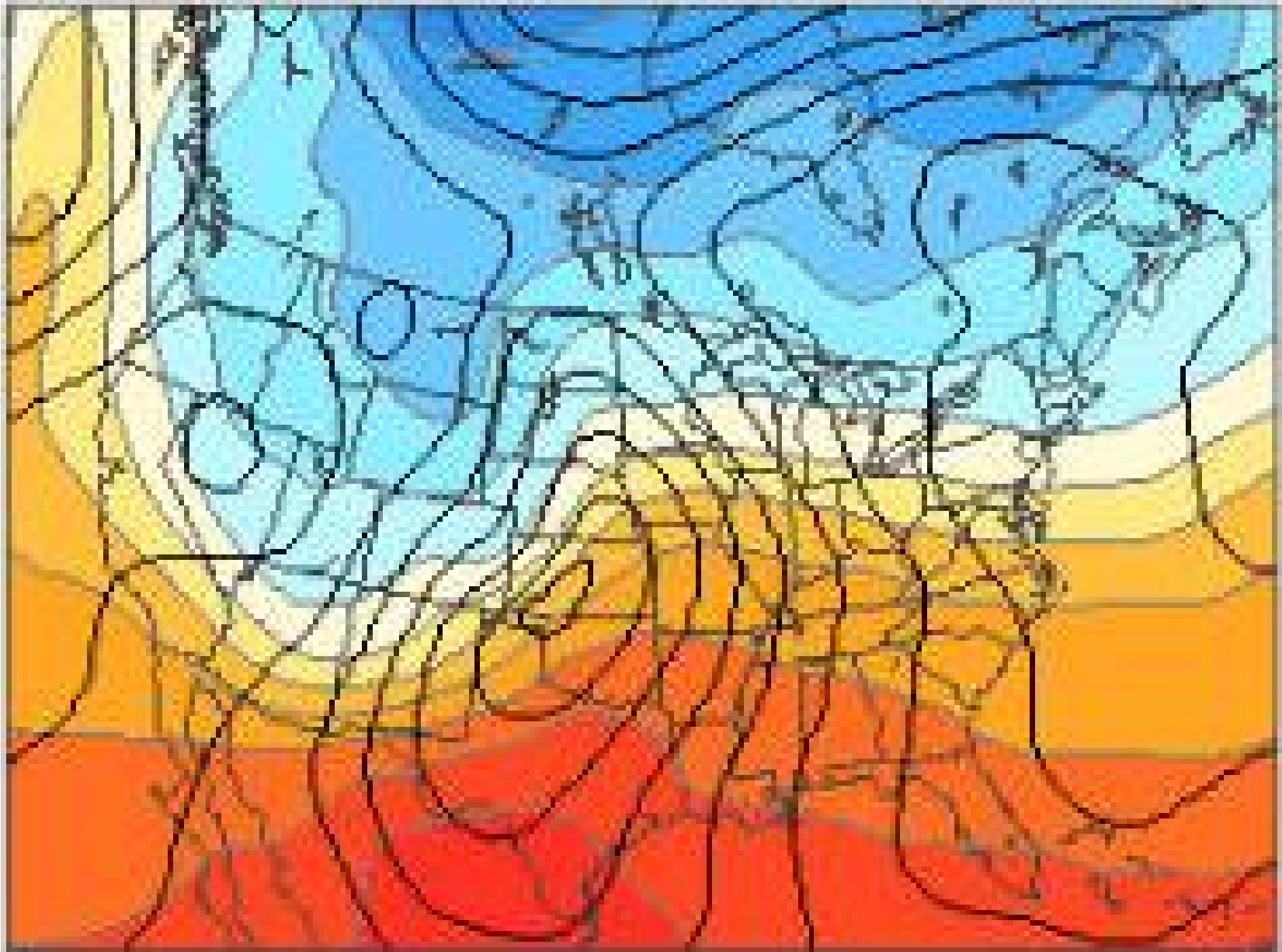
The corresponding sea level pressure and surface air temperature patterns is also shown.

The 850-hPa height gradients tend to be stronger than the gradients in sea-level pressure (or 1000-hPa height).

Stronger gradients are indicative of **higher geostrophic wind speeds**. The winds are stronger at the 850-hPa level as well.



850 hPa level chart 00Z, November 10, 1998.
(contour 30 m for height, 4°C for temperature)



Sea level pressure and 1000-500 hPA thickness
00 UTC November 10th, 1998

Based on the thermal wind equation, we know that strengthening of the westerly component of the wind from the surface to the 850-hPa level is consistent with the prevailing meridional temperature gradient in this layer, with colder air to the north.

Based on the thermal wind equation, we know that strengthening of the westerly component of the wind from the surface to the 850-hPa level is consistent with the prevailing meridional temperature gradient in this layer, with colder air to the north.

From the hypsometric equation it is readily verified that the conventional 4-hPa contour interval for plotting sea-level pressure is roughly comparable to the 30 m contour interval used for plotting 850 hPa height.

1 hPa \approx 8 metres

Based on the thermal wind equation, we know that strengthening of the westerly component of the wind from the surface to the 850-hPa level is consistent with the prevailing meridional temperature gradient in this layer, with colder air to the north.

From the hypsometric equation it is readily verified that the conventional 4-hPa contour interval for plotting sea-level pressure is roughly comparable to the 30 m contour interval used for plotting 850 hPa height.

$$1 \text{ hPa} \approx 8 \text{ metres}$$

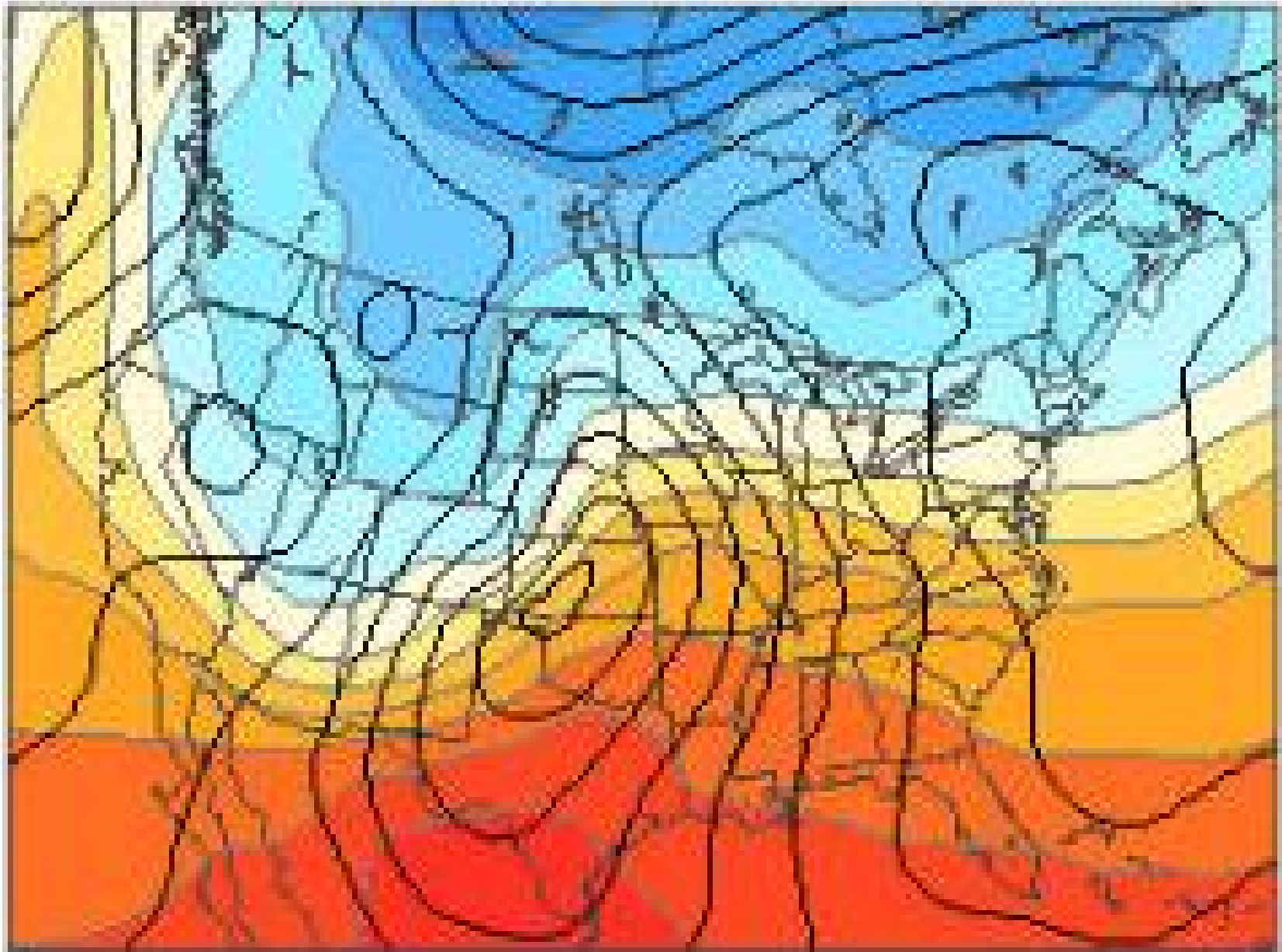
Hence, the relative strength of the pressure gradient force (and the geostrophic wind) at the two levels can be assessed qualitatively simply by comparing the spacing of the isobars and height contours.

When the differences in contour intervals in the charts is taken into account, it is seen that gradients and wind speeds **increase continuously with height** up to the 250-hPa level, which corresponds to the level of the jet stream.

When the differences in contour intervals in the charts is taken into account, it is seen that gradients and wind speeds **increase continuously with height** up to the 250-hPa level, which corresponds to the level of the jet stream.

From 250 to 100-hPa, the highest level shown, the gradients and wind speeds decrease markedly with height.





Sea level pressure and 1000-500 hPA thickness
00 UTC November 10th, 1998

The 850-hPa isotherms tend to be concentrated within the frontal zone extending from the Great Plains eastward to the Atlantic seaboard and passing through the surface low.

The 850-hPa isotherms tend to be concentrated within the frontal zone extending from the Great Plains eastward to the Atlantic seaboard and passing through the surface low.

To the east of the surface low, the winds are blowing through the frontal zone from the warm side to the cold side, advecting it northward.

To the west of the surface low they are blowing through it from the cold side to the warm side, advecting it southeastward around the southern flank of the surface low.

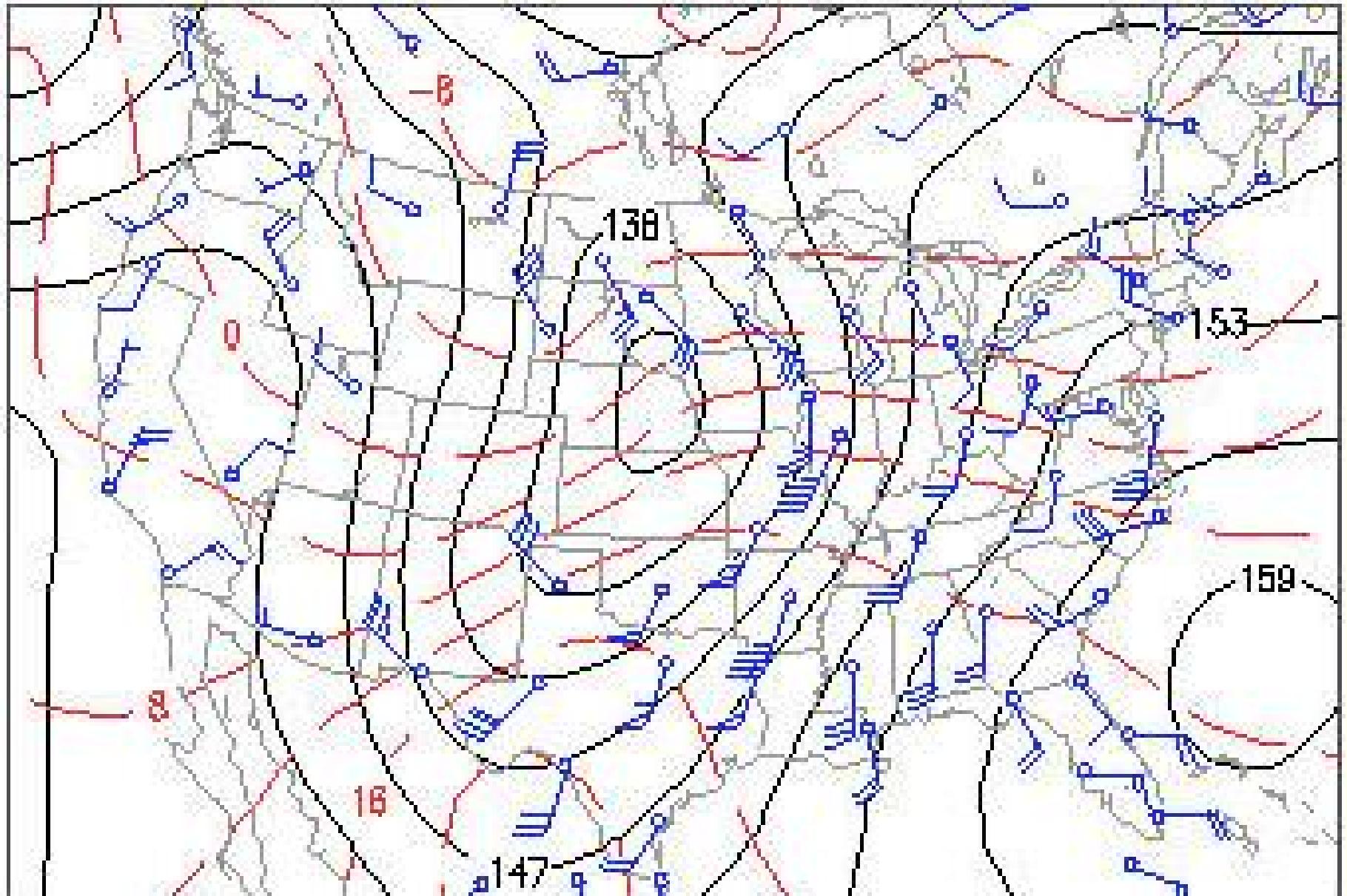
The 850-hPa isotherms tend to be concentrated within the frontal zone extending from the Great Plains eastward to the Atlantic seaboard and passing through the surface low.

To the east of the surface low, the winds are blowing through the frontal zone from the warm side to the cold side, advecting it northward.

To the west of the surface low they are blowing through it from the cold side to the warm side, advecting it southeastward around the southern flank of the surface low.

The frontal zone is particularly tight in the region of cold advection to the south of the surface low, and the temperature is fairly uniform within the warm sector to the southeast of the surface low.

The 850-hPa height contours that pass through the frontal zone exhibit **strong cyclonic curvature**.



850 hPa level chart 00Z, November 10, 1998.
(contour 30 m for height, 4°C for temperature)

Over the Carolinas, the frontal zone on the 850-hPa chart is positioned quite far to the north of its counterpart on the surface charts.

This northward displacement reflects the shallowness of the layer of trapped cool air to the east of the Appalachian mountain range.



Over the Carolinas, the frontal zone on the 850-hPa chart is positioned quite far to the north of its counterpart on the surface charts.

This northward displacement reflects the shallowness of the layer of trapped cool air to the east of the Appalachian mountain range.

★ ★ ★

Proceeding upward from the 850-hPa to the 250-hPa level, the patterns exhibit notable changes. The geopotential height gradients and the associated geostrophic winds **generally increase with height**, and this tendency is mirrored in the strength of the observed winds.

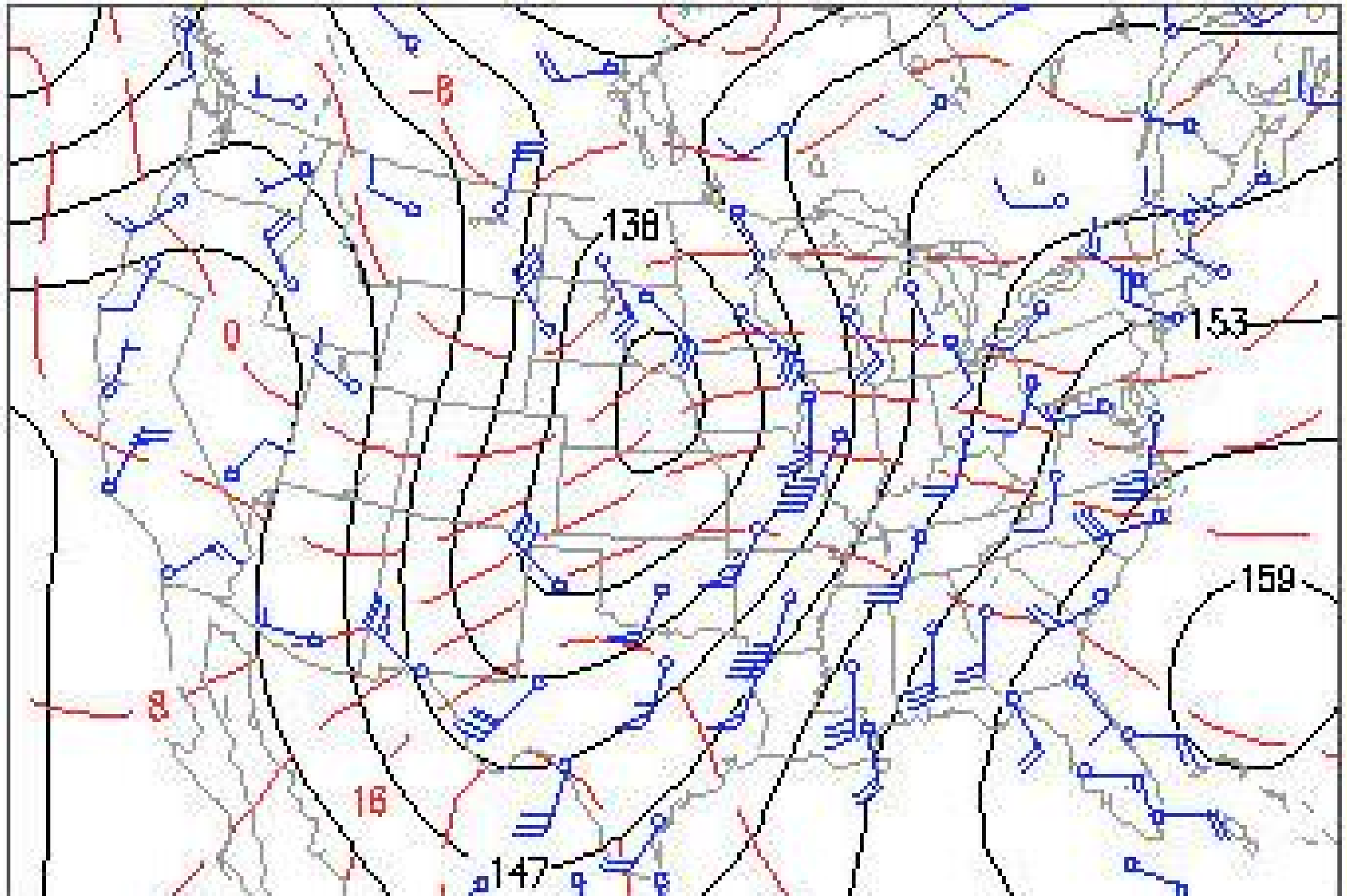
Over the Carolinas, the frontal zone on the 850-hPa chart is positioned quite far to the north of its counterpart on the surface charts.

This northward displacement reflects the shallowness of the layer of trapped cool air to the east of the Appalachian mountain range.

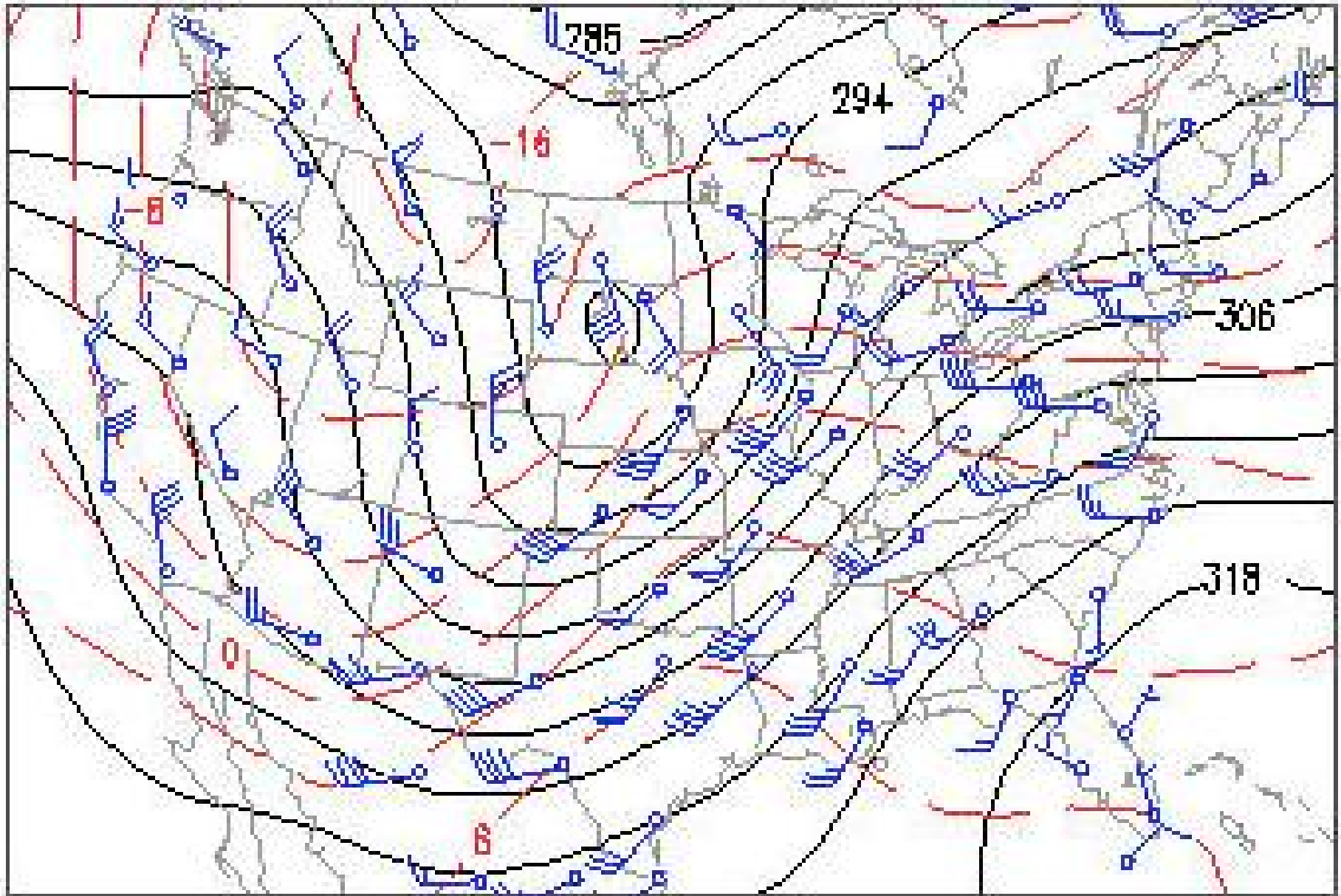
★ ★ ★

Proceeding upward from the 850-hPa to the 250-hPa level, the patterns exhibit notable changes. The geopotential height gradients and the associated geostrophic winds **generally increase with height**, and this tendency is mirrored in the strength of the observed winds.

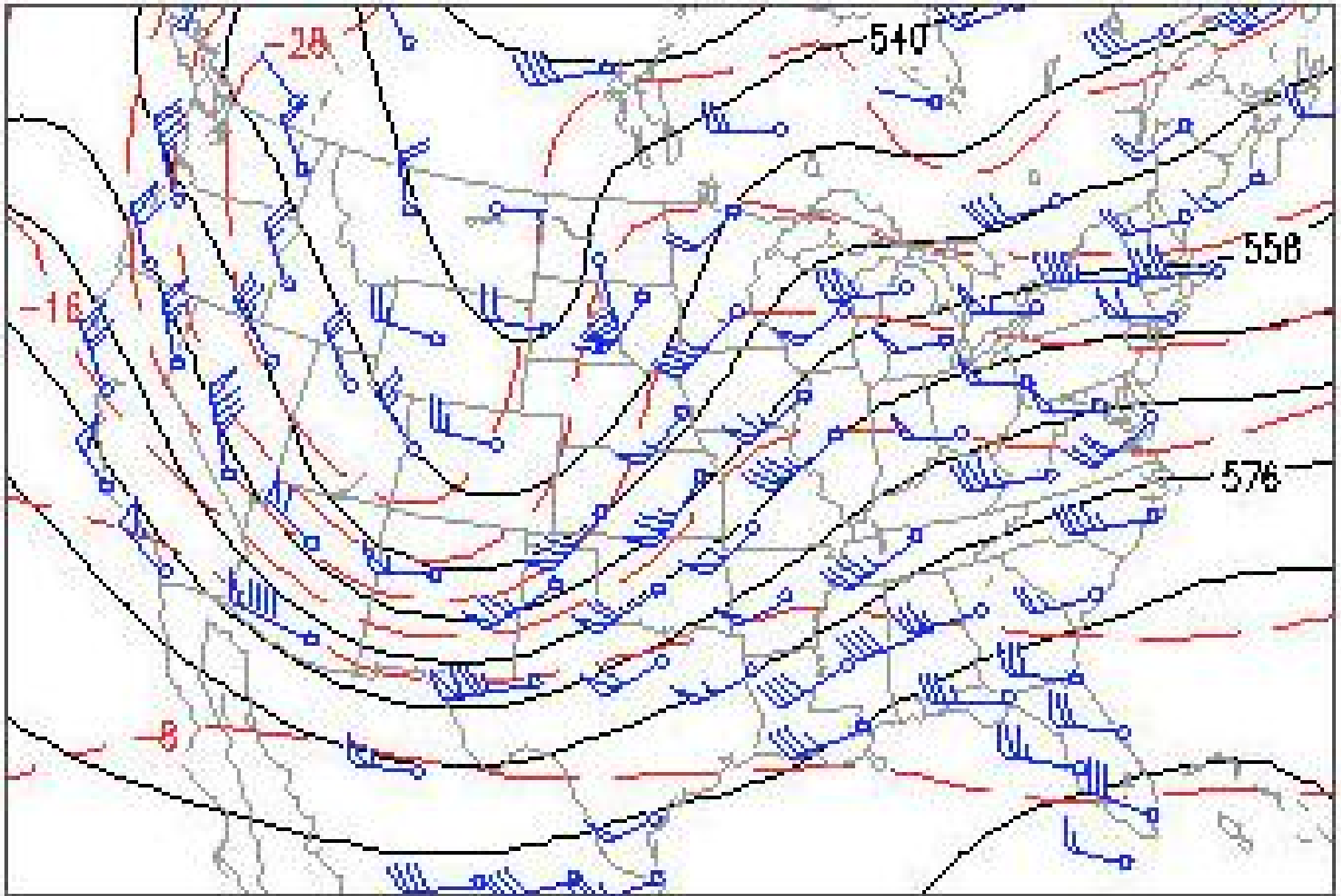
The trough in the geopotential height field tilts westward with height by around 1/4 wavelength from the surface up to the 500-hPa level, but it exhibits relatively little vertical tilt above that level.



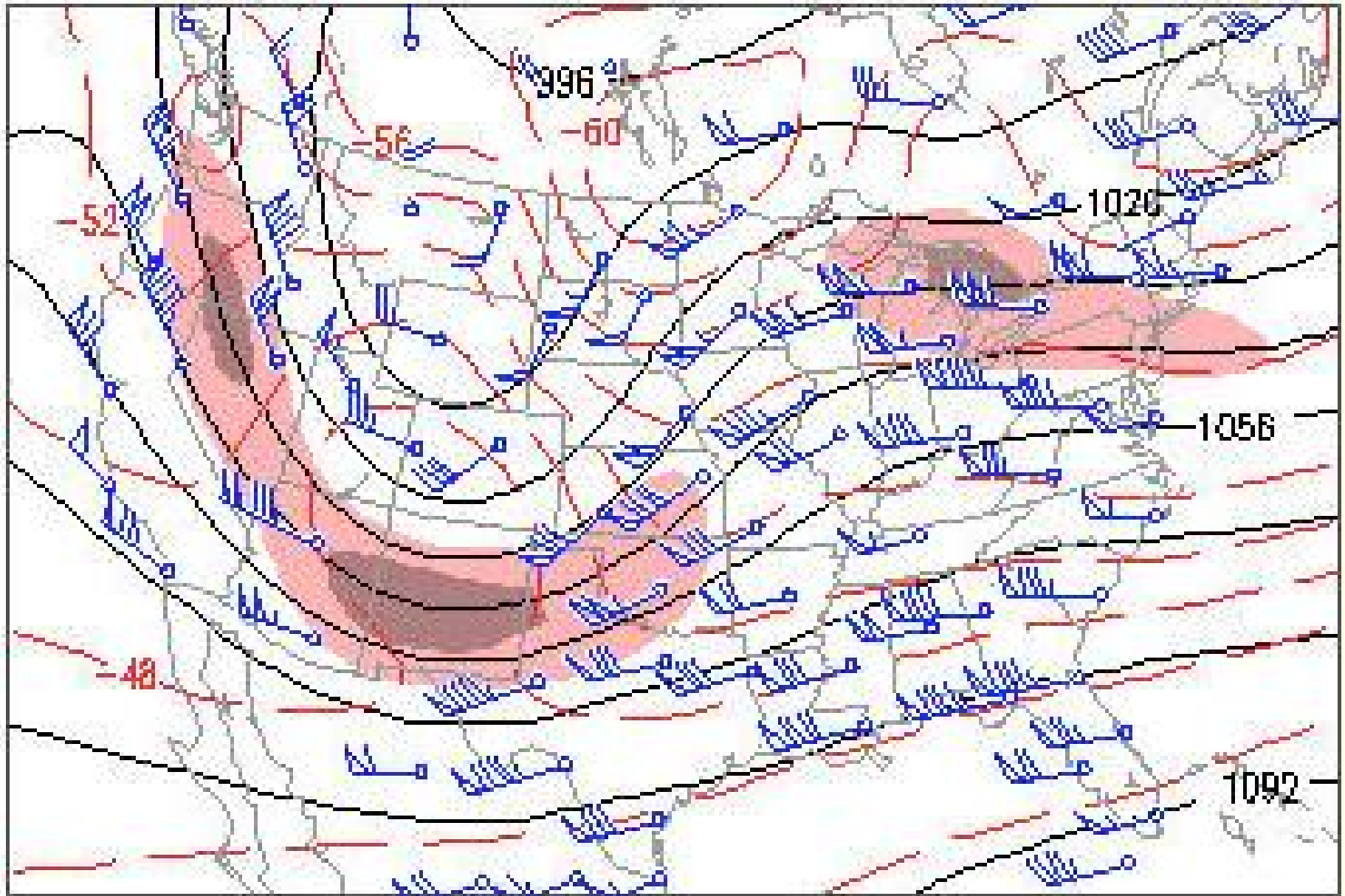
850 hPa level chart 00Z, November 10, 1998.
(contour 30 m for height, 4°C for temperature)



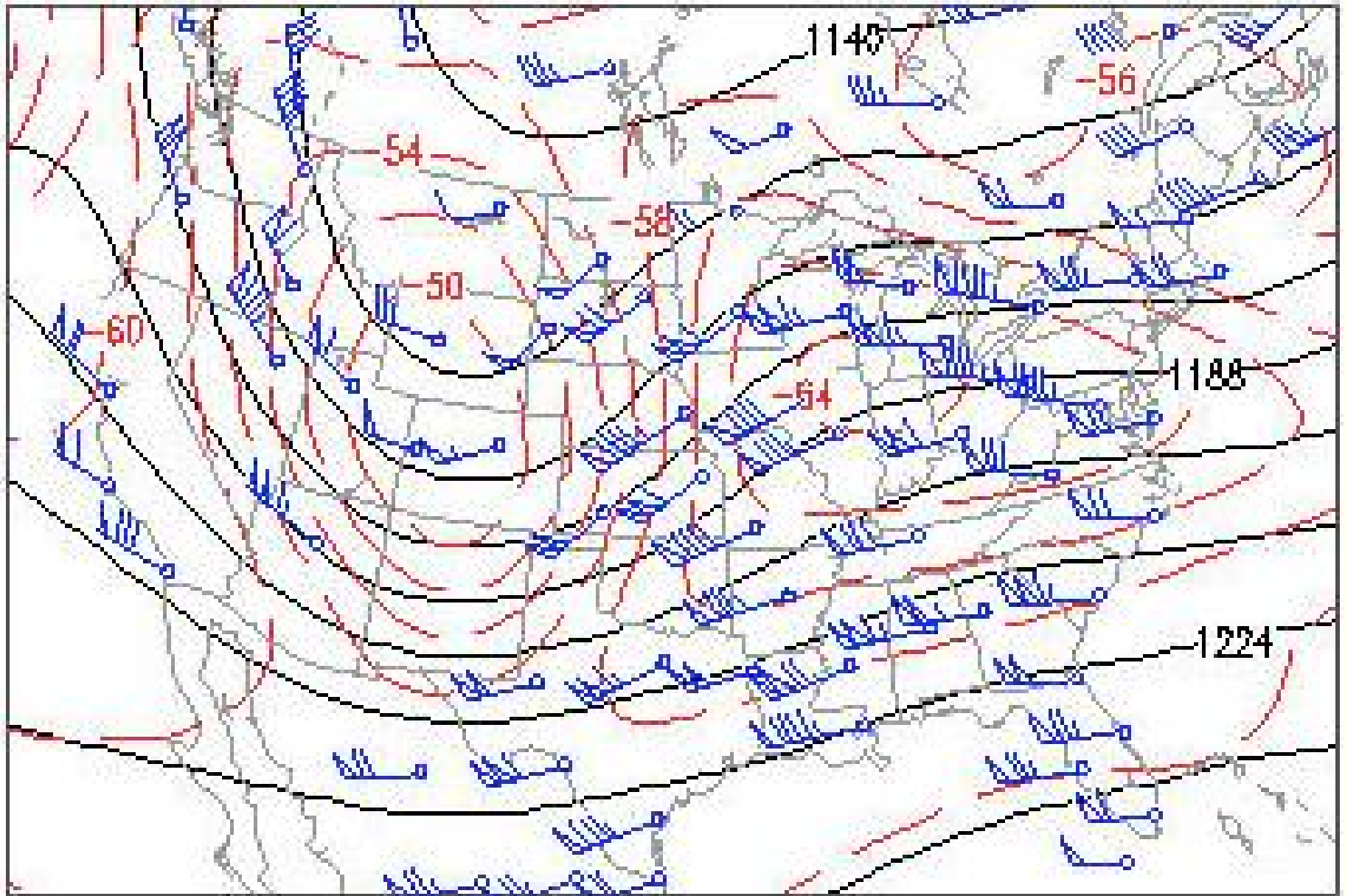
700 hPa level chart 00Z, November 10, 1998.
(contour 30 m for height, 4°C for temperature)



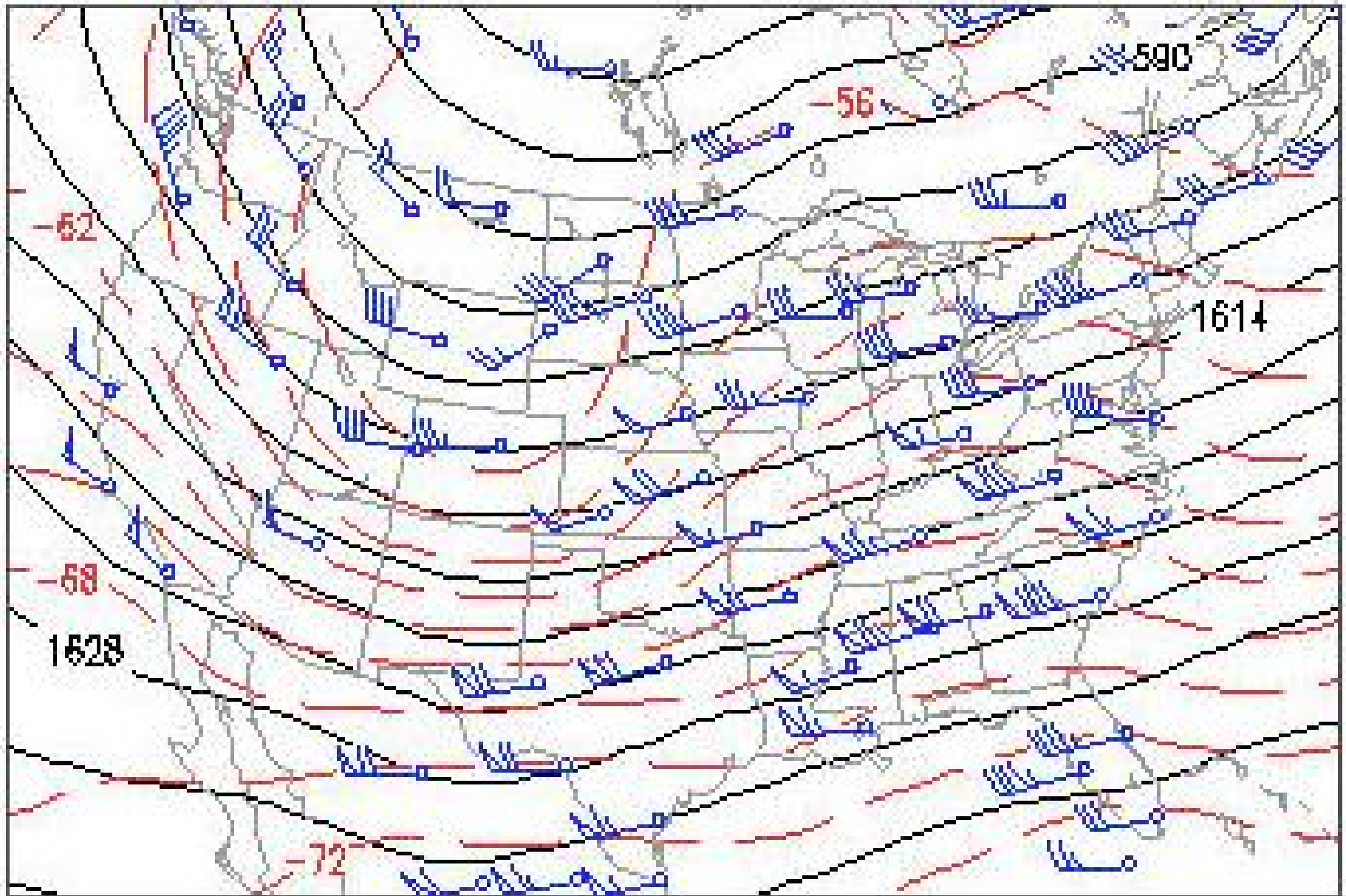
500 hPa level chart 00Z, November 10, 1998.
(contour 60 m for height, 4°C for temperature)



250 hPa level chart 00Z, November 10, 1998.
(contour 120 m for height, 2°C for temperature)



200 hPa level chart 00Z, November 10, 1998.
(contour 120 m for height, 2°C for temperature)



100 hPa level chart 00Z, November 10, 1998.
(contour 60 m for height, 2°C for temperature)

The horizontal temperature advection also weakens with height as the wind vectors come into alignment with the isotherms. In contrast to the patterns at 850 and 700-hPa, which are highly baroclinic, the structure at the higher levels is more **equivalent barotropic**.

The horizontal temperature advection also weakens with height as the wind vectors come into alignment with the isotherms. In contrast to the patterns at 850 and 700-hPa, which are highly baroclinic, the structure at the higher levels is more **equivalent barotropic**.

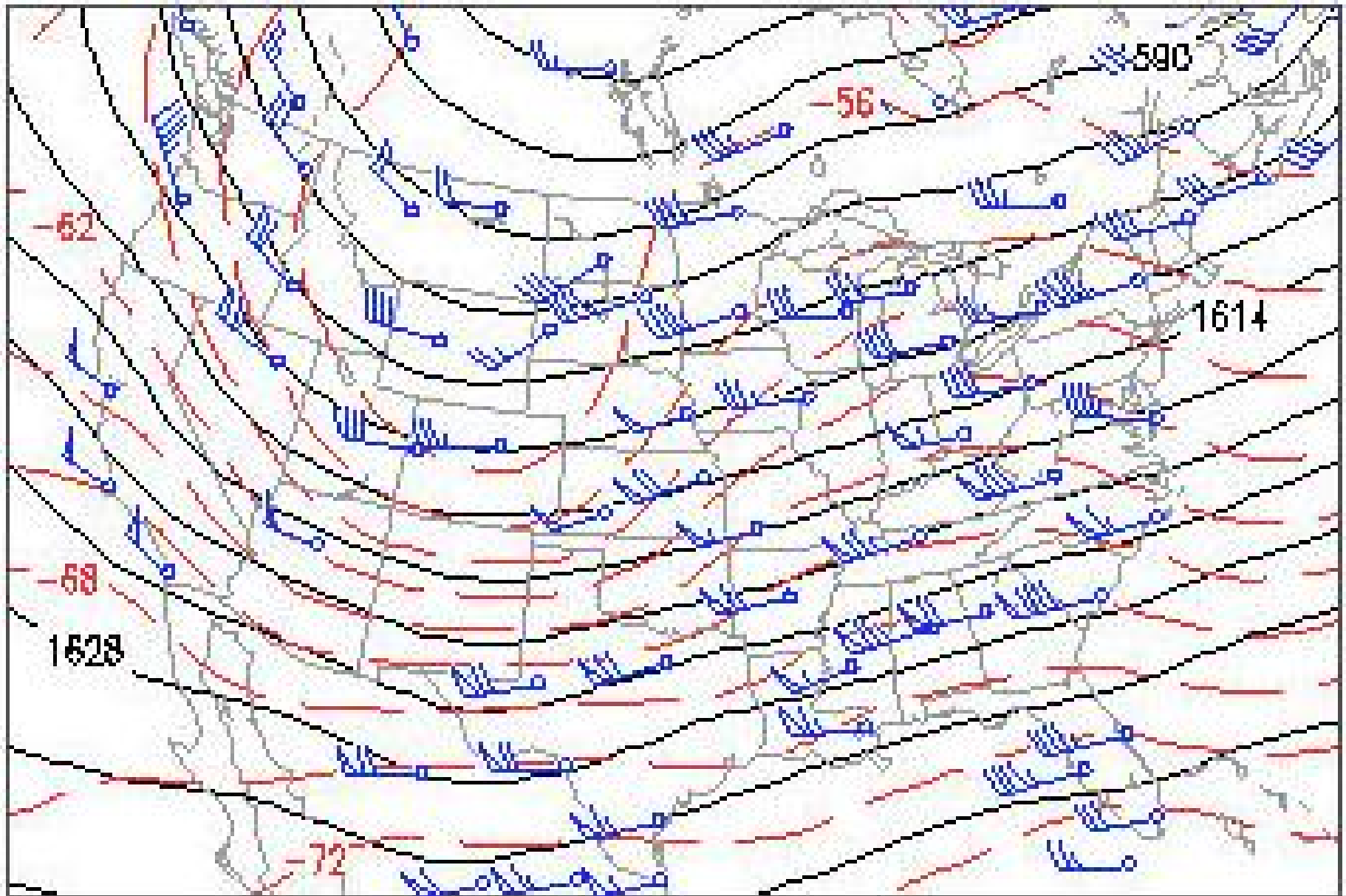
The temperature patterns in the lower stratosphere are weak and are entirely different from those in the troposphere. At these levels, the air in troughs in the geopotential height field tends to be **warmer** than the surrounding air, and the air in ridges tends to be cold.

The horizontal temperature advection also weakens with height as the wind vectors come into alignment with the isotherms. In contrast to the patterns at 850 and 700-hPa, which are highly baroclinic, the structure at the higher levels is more **equivalent barotropic**.

The temperature patterns in the lower stratosphere are weak and are entirely different from those in the troposphere. At these levels, the air in troughs in the geopotential height field tends to be **warmer** than the surrounding air, and the air in ridges tends to be cold.

From the hypsometric equation it follows that the amplitudes of the ridges and troughs must decrease with height, consistent with the observations.

By the time we reach the 100 hPa level, the only vestige of the baroclinic wave that remains is the weak trough over the western United States.



100 hPa level chart 00Z, November 10, 1998.
(contour 60 m for height, 2°C for temperature)

The 250-hPa height contours, indicative of the flow at the **jet stream level** are seen to be aligned with the isotherms in the lower tropospheric temperature field.

The 250-hPa height contours, indicative of the flow at the **jet stream level** are seen to be aligned with the isotherms in the lower tropospheric temperature field.

The jet stream passes over the baroclinic zones, with colder air lying to the left of it.

★ ★ ★

The 250-hPa height contours, indicative of the flow at the **jet stream level** are seen to be aligned with the isotherms in the lower tropospheric temperature field.

The jet stream passes over the baroclinic zones, with colder air lying to the left of it.

★ ★ ★

The cold air in the trough of the wave in the western United States was subsiding and spreading out at the earth's surface, as reflected in the rapid advance of the cold front.

The subsidence of the cold air depressed the tropopause and adiabatically warmed the air in the lower stratosphere.

The tropopause was located below the 300-hPa (~ 9 km) level at stations in the trough region, and tropopause temperatures were near -50°C .

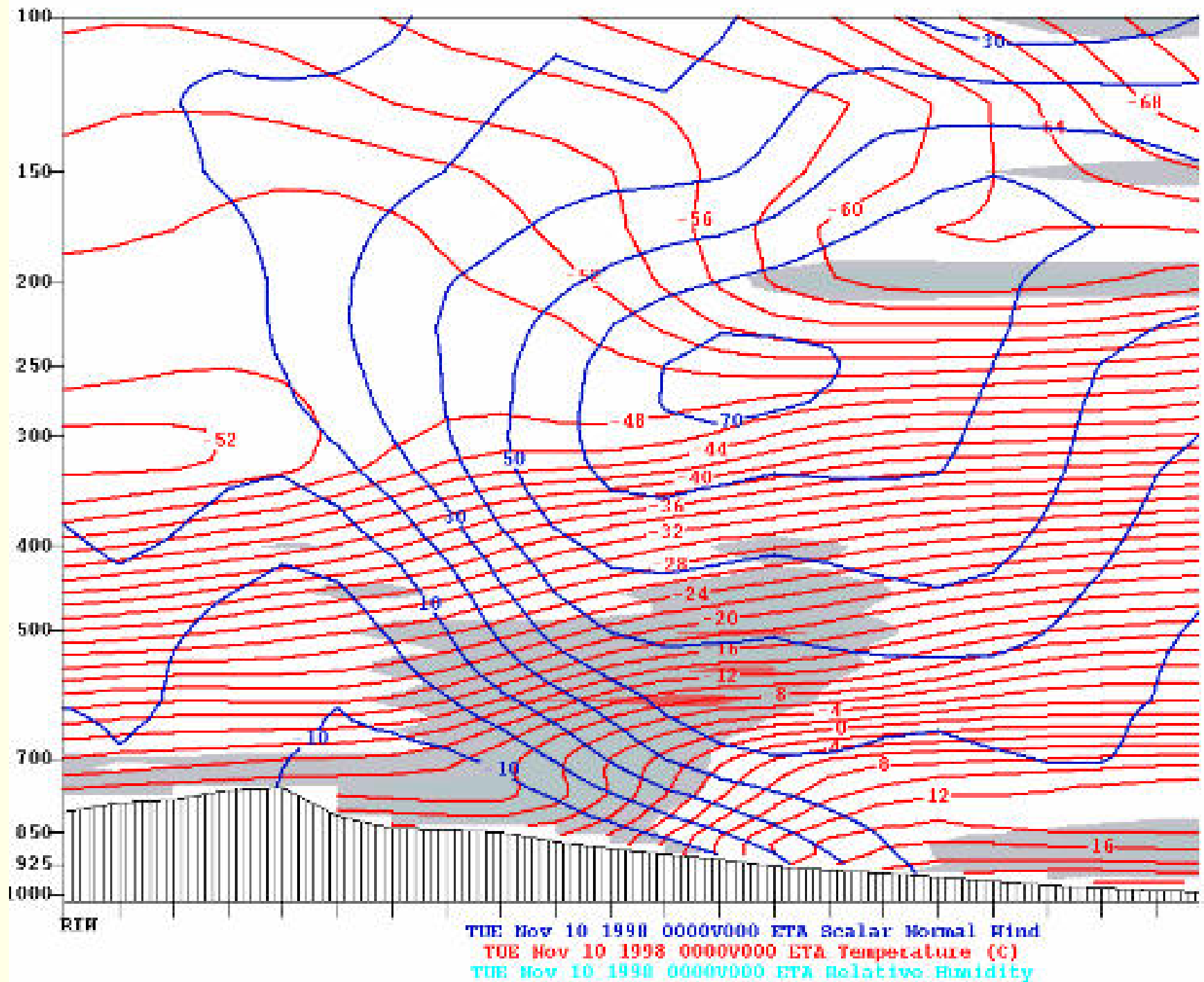
The tropopause was located below the 300-hPa (~ 9 km) level at stations in the trough region, and tropopause temperatures were near -50°C .

At the 250-hPa level, relative humidities over the center of the trough were in the 25–40% range, indicative of a recent history of subsidence.

The tropopause was located below the 300-hPa (~ 9 km) level at stations in the trough region, and tropopause temperatures were near -50°C .

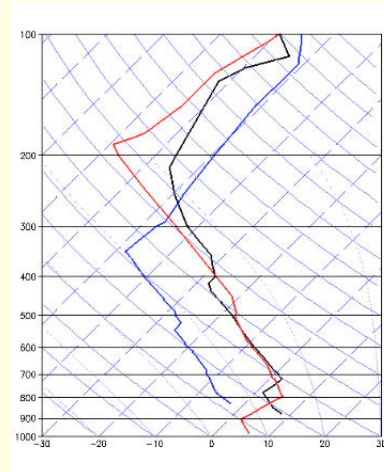
At the 250-hPa level, relative humidities over the center of the trough were in the 25–40% range, indicative of a recent history of subsidence.

Meanwhile, in the relatively warm, ascending air mass over the northern Great Plains, tropopause was above the 200 hPa (~ 12 km) level, temperatures reported at that level were below -60°C , and relative humidities were in the around 80%.

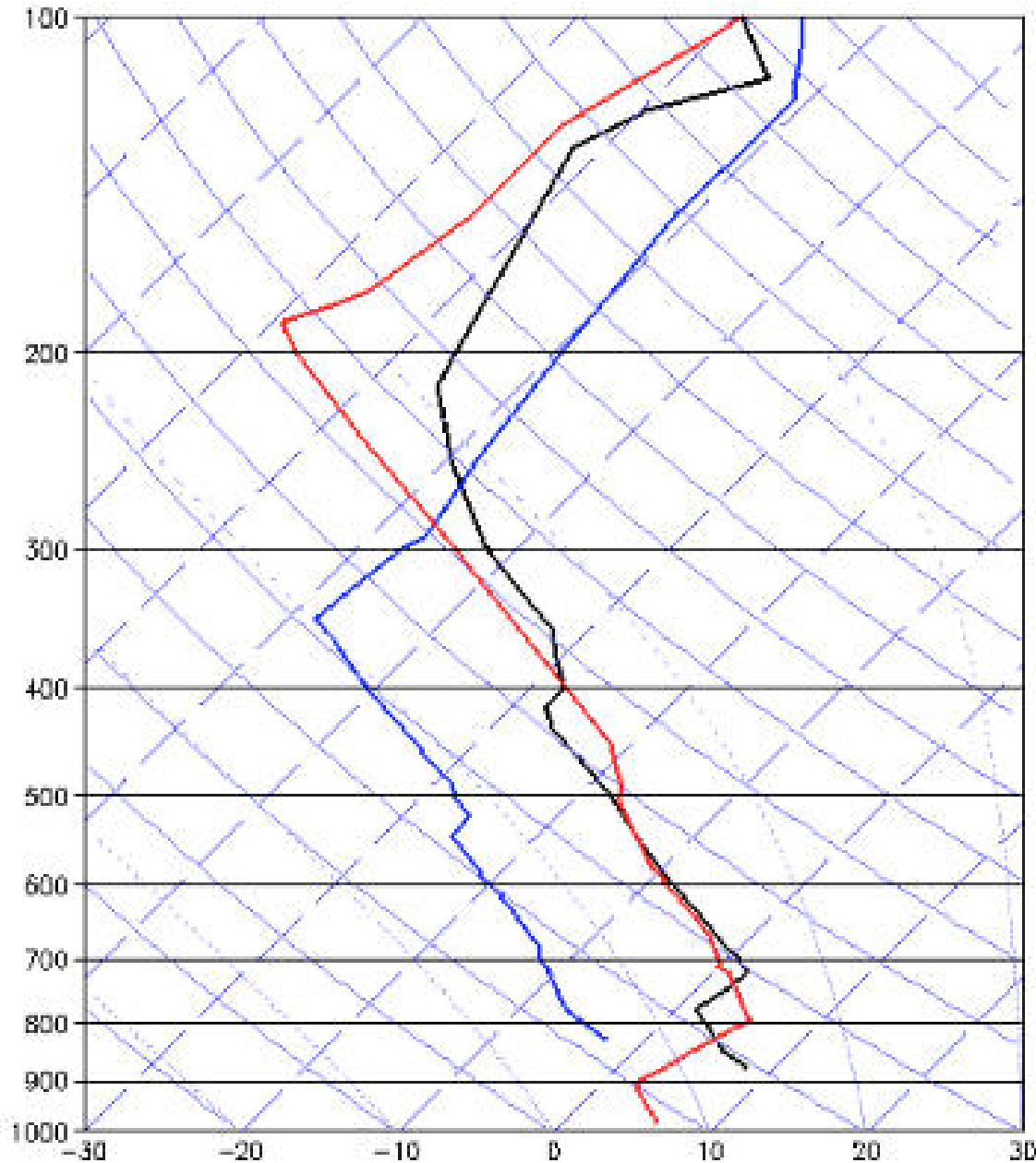


Vertical Profiles

Vertical temperature profiles for stations in the trough and ridge of the wave are contrasted in the composite diagram below.



- Denver, Colorado lies within the subsiding cold air mass near the center of the 250-hPa trough.
- Amarillo, Texas lies along the axis of the jet stream
- Davenport, Iowa lies in the region of ascent in the ridge at the jet stream level.



Vertical temperature profiles for
Denver (blue)
Amarillo (black) and
Davenport (red),
00 UTC, 10 Nov. 1998
(skew-T ln p diagram).

The Denver, Colorado profile, near the center of the 250-hPa trough is relatively cold at tropospheric levels. It exhibits a distinct discontinuity in lapse-rate around the 350 hPa (8 km) level, with a transition to more isothermal conditions.

The Denver, Colorado profile, near the center of the 250-hPa trough is relatively cold at tropospheric levels. It exhibits a distinct discontinuity in lapse-rate around the 350 hPa (8 km) level, with a transition to more isothermal conditions.

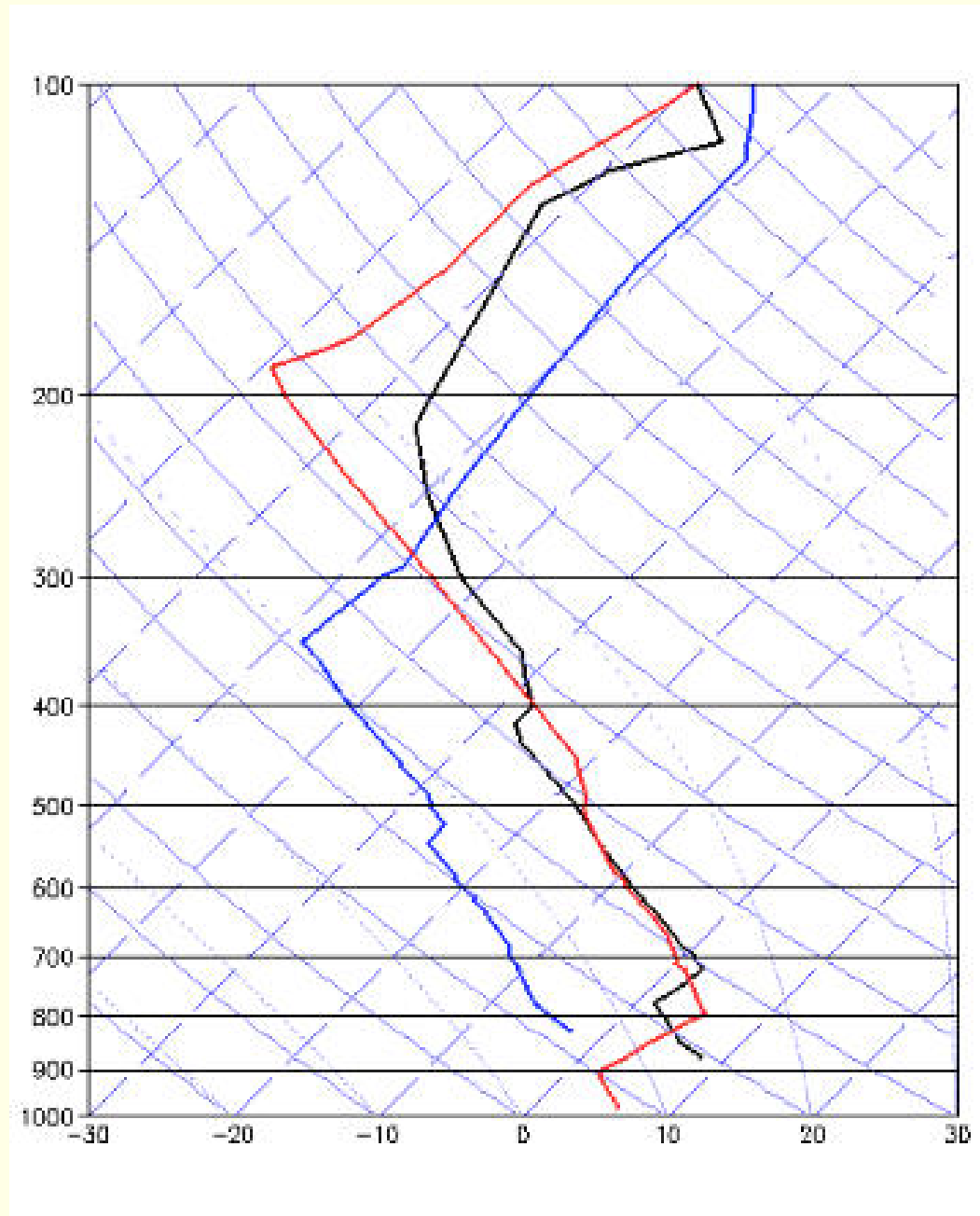
In contrast, the Davenport, Iowa profile exhibits a much colder and more distinctive tropopause at the 180-hPa (12.5 km) level. The tropopause temperature at this time was 20°C colder at Davenport than at Denver.

The Denver, Colorado profile, near the center of the 250-hPa trough is relatively cold at tropospheric levels. It exhibits a distinct discontinuity in lapse-rate around the 350 hPa (8 km) level, with a transition to more isothermal conditions.

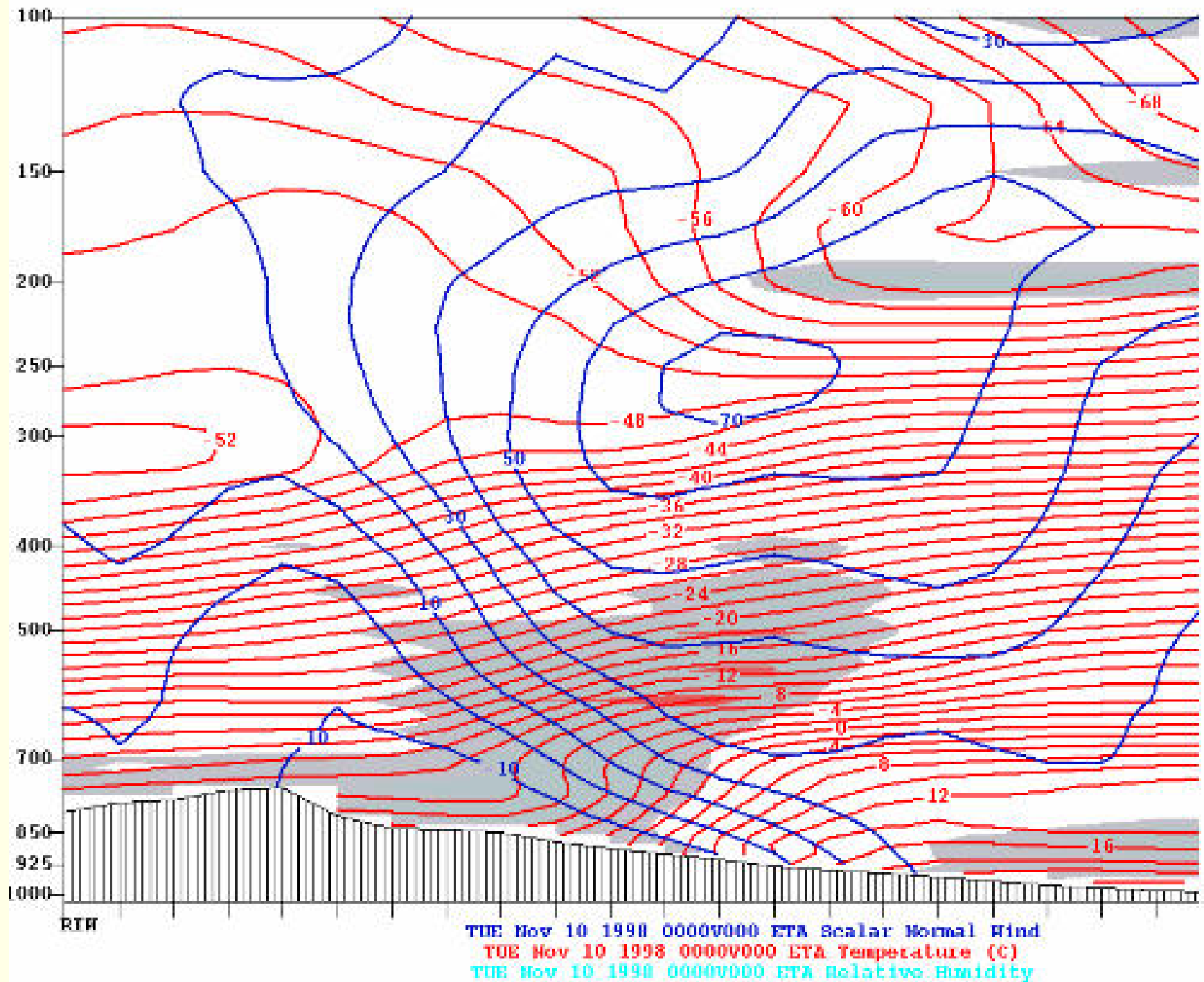
In contrast, the Davenport, Iowa profile exhibits a much colder and more distinctive tropopause at the 180-hPa (12.5 km) level. The tropopause temperature at this time was 20°C colder at Davenport than at Denver.

Amarillo, Texas, which lies close to the axis of the jet stream exhibits a less clearly defined tropopause structure, with no indications of a clear break in the lapse rate.

Along the axis of the jet stream the tropopause is not so much a layer as a vertical wall, with stratospheric air to the left and tropospheric air to the right (in the northern hemisphere).



Denver (blue), Amarillo (black) and Davenport (red).



Soundings

We next examine vertical profiles of wind, temperature and dew point in the lower troposphere at representative stations in different sectors of the developing cyclone.

Soundings

We next examine vertical profiles of wind, temperature and dew point in the lower troposphere at representative stations in different sectors of the developing cyclone.

At Amarillo (Texas), to the south of the surface low, the 850-hPa level lies within a relatively thin layer in which the wind is *backing* with height (turning from northwesterly below to southwesterly above).

Soundings

We next examine vertical profiles of wind, temperature and dew point in the lower troposphere at representative stations in different sectors of the developing cyclone.

At Amarillo (Texas), to the south of the surface low, the 850-hPa level lies within a relatively thin layer in which the wind is *backing* with height (turning from northwesterly below to southwesterly above).

From the thermal wind equation, **strong backing implies strong cold advection.**

Soundings

We next examine vertical profiles of wind, temperature and dew point in the lower troposphere at representative stations in different sectors of the developing cyclone.

At Amarillo (Texas), to the south of the surface low, the 850-hPa level lies within a relatively thin layer in which the wind is *backing* with height (turning from northwesterly below to southwesterly above).

From the thermal wind equation, **strong backing implies strong cold advection.**

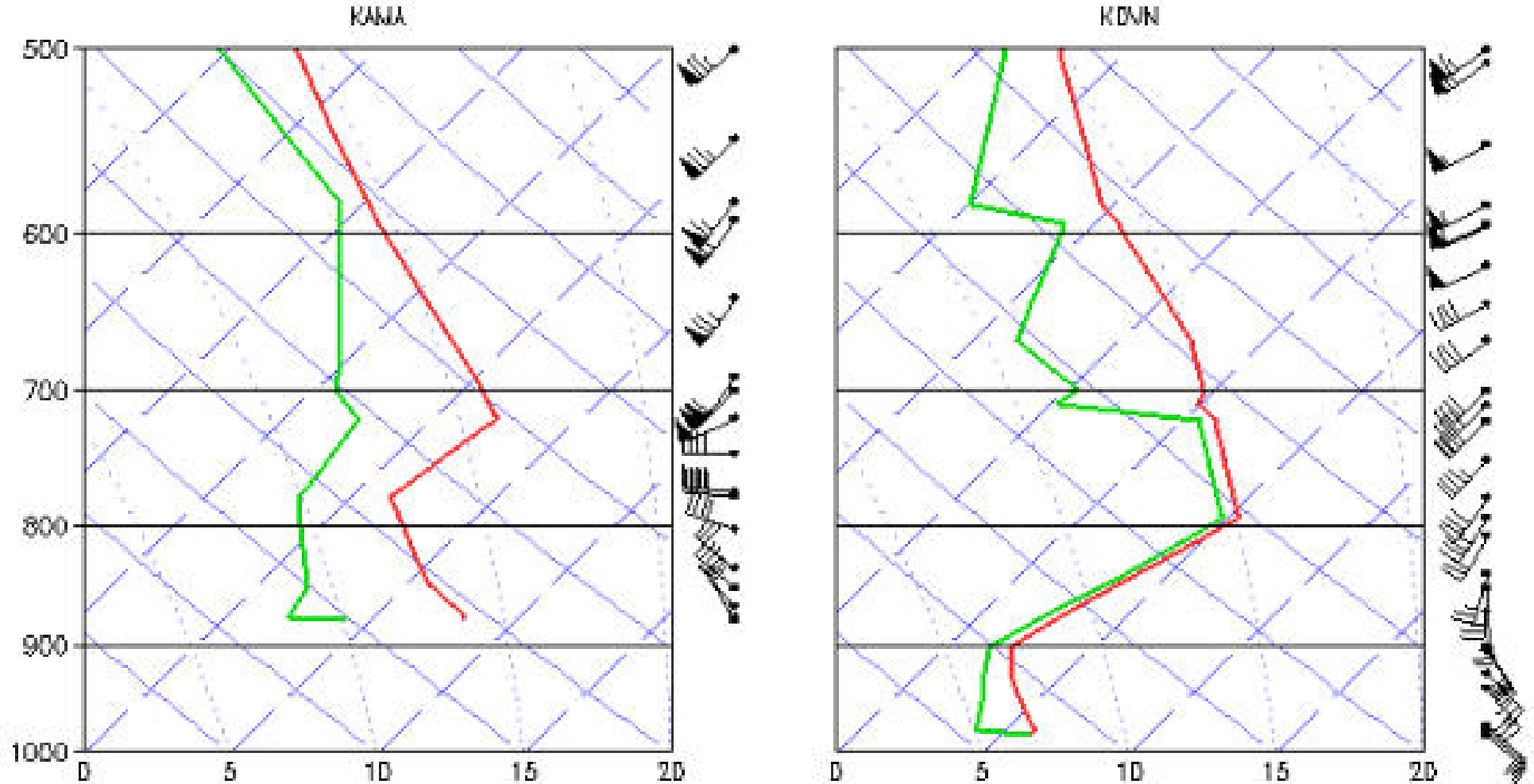
[Recall:

$$\mathbf{V}_g = \frac{1}{f} \mathbf{k} \times \nabla \Phi \quad \Longrightarrow \quad \frac{\partial \mathbf{V}_g}{\partial p} = \frac{1}{f} \mathbf{k} \times \nabla \frac{\partial \Phi}{\partial p} \propto -\mathbf{k} \times \nabla T$$

so

$$\frac{\partial \mathbf{V}_g}{\partial z} \propto \mathbf{k} \times \nabla T$$

so the cold air is to the left of the shear-vector.]



Soundings of wind, temperature and dew point at 00 UTC, November 20, 1998. *Left:* Amarillo, Texas in the cold frontal zone; *Right:* Davenport, Iowa in the warm frontal zone.

The positioning of this layer of strong backing just above the 850-hPa level in the sounding indicates that the frontal zone lies just to the east of Amarillo and that it slopes westward with height.



The positioning of this layer of strong backing just above the 850-hPa level in the sounding indicates that the frontal zone lies just to the east of Amarillo and that it slopes westward with height.

★ ★ ★

The sounding for Davenport lies on the cold side of the frontal zone to the east of the surface low, where the warm air is being advected northward by the southerly component of the wind.

In the Davenport sounding, the wind *veers* with increasing height, indicative of warm advection.

The positioning of this layer of strong backing just above the 850-hPa level in the sounding indicates that the frontal zone lies just to the east of Amarillo and that it slopes westward with height.

★ ★ ★

The sounding for Davenport lies on the cold side of the frontal zone to the east of the surface low, where the warm air is being advected northward by the southerly component of the wind.

In the Davenport sounding, the wind *veers* with increasing height, indicative of warm advection.

Soundings for stations located in the warm sector of the developing cyclone (not shown) exhibit little turning of wind with height other than the frictional veering just above the surface, and relatively little increase of wind speed with height.

Vertical Cross-sections

Vertical cross-sections are the natural complement to horizontal maps in revealing the three-dimensional structure of weather systems.

Vertical Cross-sections

Vertical cross-sections are the natural complement to horizontal maps in revealing the three-dimensional structure of weather systems.

With today's high resolution gridded data sets generated by sophisticated data assimilation schemes, all the analyst need do is specify the time and orientation of the section and the fields to be included in the section.

Vertical Cross-sections

Vertical cross-sections are the natural complement to horizontal maps in revealing the three-dimensional structure of weather systems.

With today's high resolution gridded data sets generated by sophisticated data assimilation schemes, all the analyst need do is specify the time and orientation of the section and the fields to be included in the section.

The two most widely used variables in vertical cross sections are temperature (or equivalent potential temperature) and wind.

Vertical Cross-sections

Vertical cross-sections are the natural complement to horizontal maps in revealing the three-dimensional structure of weather systems.

With today's high resolution gridded data sets generated by sophisticated data assimilation schemes, all the analyst need do is specify the time and orientation of the section and the fields to be included in the section.

The two most widely used variables in vertical cross sections are temperature (or equivalent potential temperature) and wind.

If the plane of the section is oriented normal to the jet stream, the analysis can be simplified by resolving the wind into components parallel and normal to the section.

Isotachs of the normal component clearly reveal the location and strength of the jet stream where it passes through the plane of the section and they often capture the zones of strongest vertical wind shear, where patches of clear air turbulence tend to be concentrated.

Isotachs of the normal component clearly reveal the location and strength of the jet stream where it passes through the plane of the section and they often capture the zones of strongest vertical wind shear, where patches of clear air turbulence tend to be concentrated.

The vertical shear of the wind component normal to the section and the horizontal temperature gradient along the section are approximately related by the **thermal wind equation**:

$$\frac{\partial V_n}{\partial p} \approx -\frac{R}{f p} \frac{\partial T}{\partial s}$$

where V_n is the wind component into the section and T is temperature in the plane of the section, with the horizontal coordinate s increasing toward the right.

Isotachs of the normal component clearly reveal the location and strength of the jet stream where it passes through the plane of the section and they often capture the zones of strongest vertical wind shear, where patches of clear air turbulence tend to be concentrated.

The vertical shear of the wind component normal to the section and the horizontal temperature gradient along the section are approximately related by the **thermal wind equation**:

$$\frac{\partial V_n}{\partial p} \approx -\frac{R}{f p} \frac{\partial T}{\partial s}$$

where V_n is the wind component into the section and T is temperature in the plane of the section, with the horizontal coordinate s increasing toward the right.

It follows that ...

- In regions of the section in which the flow is *barotropic*, isotherms are horizontal ($\partial T/\partial s = 0$) and isotachs are vertical ($\partial V_n/\partial p = 0$).

- In regions of the section in which the flow is *barotropic*, isotherms are horizontal ($\partial T/\partial s = 0$) and isotachs are vertical ($\partial V_n/\partial p = 0$).
- In regions where isotachs are tightly spaced in the vertical, isotherms are tightly spaced in the horizontal.

- In regions of the section in which the flow is *barotropic*, isotherms are horizontal ($\partial T/\partial s = 0$) and isotachs are vertical ($\partial V_n/\partial p = 0$).
- In regions where isotachs are tightly spaced in the vertical, isotherms are tightly spaced in the horizontal.
- Near the tropopause, the vertical wind shear and the horizontal temperature gradient undergo a sign reversal at the same level.

- In regions of the section in which the flow is *barotropic*, isotherms are horizontal ($\partial T/\partial s = 0$) and isotachs are vertical ($\partial V_n/\partial p = 0$).
- In regions where isotachs are tightly spaced in the vertical, isotherms are tightly spaced in the horizontal.
- Near the tropopause, the vertical wind shear and the horizontal temperature gradient undergo a sign reversal at the same level.

The same relationships apply to vertical wind shear and the horizontal gradient of potential temperature.

- In regions of the section in which the flow is *barotropic*, isotherms are horizontal ($\partial T/\partial s = 0$) and isotachs are vertical ($\partial V_n/\partial p = 0$).
- In regions where isotachs are tightly spaced in the vertical, isotherms are tightly spaced in the horizontal.
- Near the tropopause, the vertical wind shear and the horizontal temperature gradient undergo a sign reversal at the same level.

The same relationships apply to vertical wind shear and the horizontal gradient of potential temperature.

Temperature and **potential temperature** sections are different in appearance:

- In regions of the section in which the flow is *barotropic*, isotherms are horizontal ($\partial T/\partial s = 0$) and isotachs are vertical ($\partial V_n/\partial p = 0$).
- In regions where isotachs are tightly spaced in the vertical, isotherms are tightly spaced in the horizontal.
- Near the tropopause, the vertical wind shear and the horizontal temperature gradient undergo a sign reversal at the same level.

The same relationships apply to vertical wind shear and the horizontal gradient of potential temperature.

Temperature and **potential temperature** sections are different in appearance:

- in the troposphere temperature usually decreases with height while potential temperature increases with height

- In regions of the section in which the flow is *barotropic*, isotherms are horizontal ($\partial T/\partial s = 0$) and isotachs are vertical ($\partial V_n/\partial p = 0$).
- In regions where isotachs are tightly spaced in the vertical, isotherms are tightly spaced in the horizontal.
- Near the tropopause, the vertical wind shear and the horizontal temperature gradient undergo a sign reversal at the same level.

The same relationships apply to vertical wind shear and the horizontal gradient of potential temperature.

Temperature and **potential temperature** sections are different in appearance:

- in the troposphere temperature usually decreases with height while potential temperature increases with height
- in the stratosphere $\partial\theta/\partial p$ is always strong and negative, while $\partial T/\partial p$ is often weak and may be of either sign.

First vertical cross-section

The first example is oriented perpendicular to the cold front and jet stream over the southern Great Plains, 00 UTC 10 November 1998, looking downstream (i.e., northeastward).

First vertical cross-section

The first example is oriented perpendicular to the cold front and jet stream over the southern Great Plains, 00 UTC 10 November 1998, looking downstream (i.e., northeastward).

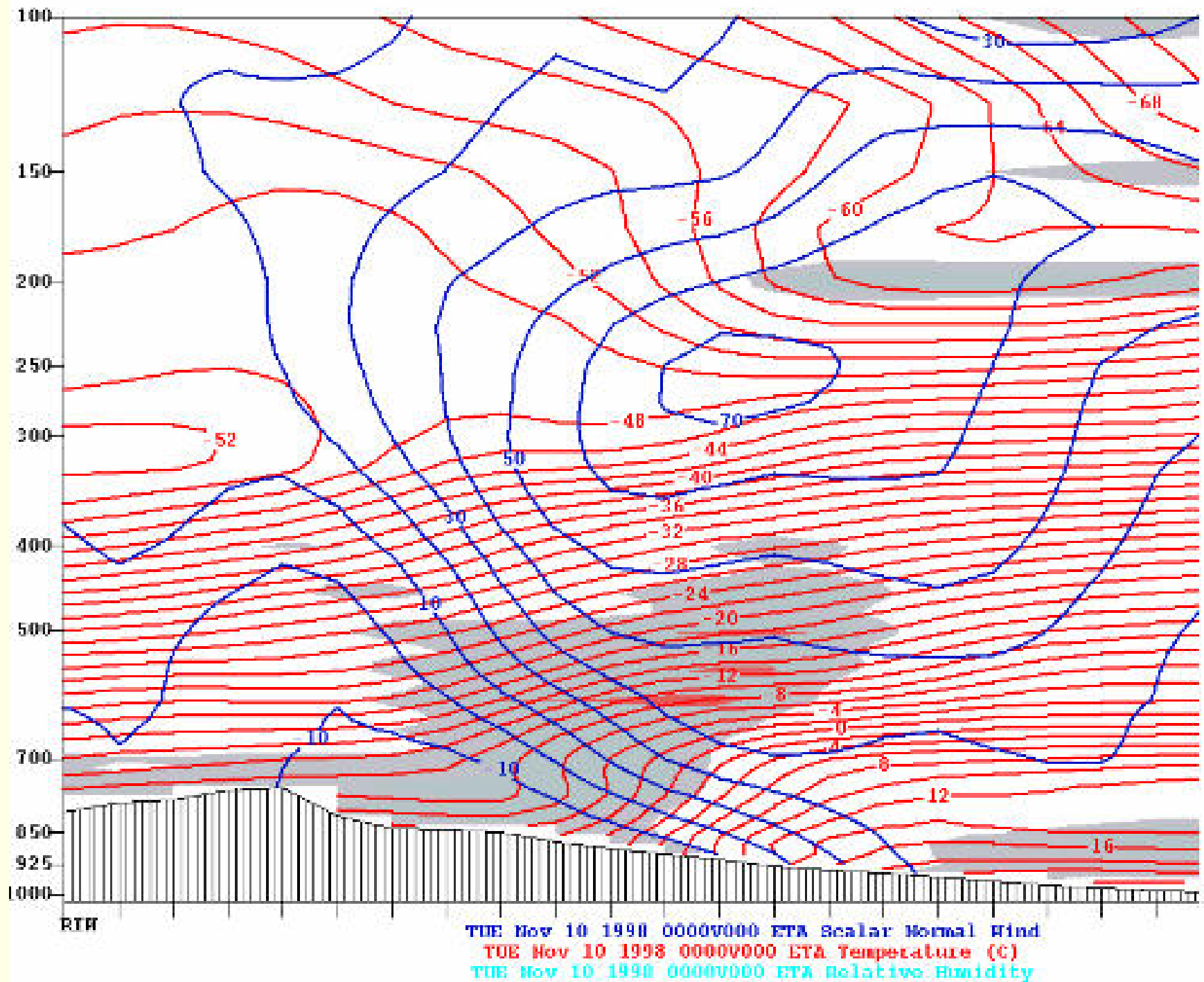
Temperature is indicated by **red** contours and isotachs of geostrophic wind speed normal to the section, with positive values defined as southwesterly winds directed into the section, are plotted in blue. Regions with relative humidities in excess of 80% are shaded.

First vertical cross-section

The first example is oriented perpendicular to the cold front and jet stream over the southern Great Plains, 00 UTC 10 November 1998, looking downstream (i.e., northeastward).

Temperature is indicated by **red** contours and isotachs of geostrophic wind speed normal to the section, with positive values defined as southwesterly winds directed into the section, are plotted in blue. Regions with relative humidities in excess of 80% are shaded.

The front at the earth's surface is apparent as a wedge of downward sloping isotherms and strong vertical wind shear, as indicated by the close spacing of the isotachs in the vertical.



The front slopes backward toward the cold air, with increasing height. The front becomes less clearly defined at levels above 850 hPa.

The front slopes backward toward the cold air, with increasing height. The front becomes less clearly defined at levels above 850 hPa.

The jet stream passes through the section at the 250-hPa level, directly above the frontal zone.

The wind speed in the core of the jet stream is slightly in excess of 70 m/s.

The front slopes backward toward the cold air, with increasing height. The front becomes less clearly defined at levels above 850 hPa.

The jet stream passes through the section at the 250-hPa level, directly above the frontal zone.

The wind speed in the core of the jet stream is slightly in excess of 70 m/s.

The tropopause is clearly evident as a discontinuity in the vertical spacing of the isotherms: in the troposphere the isotherms are closely spaced in the vertical, indicative of strong lapse rates, while in the stratosphere, they are widely spaced, indicative of close-to-isothermal lapse rates.

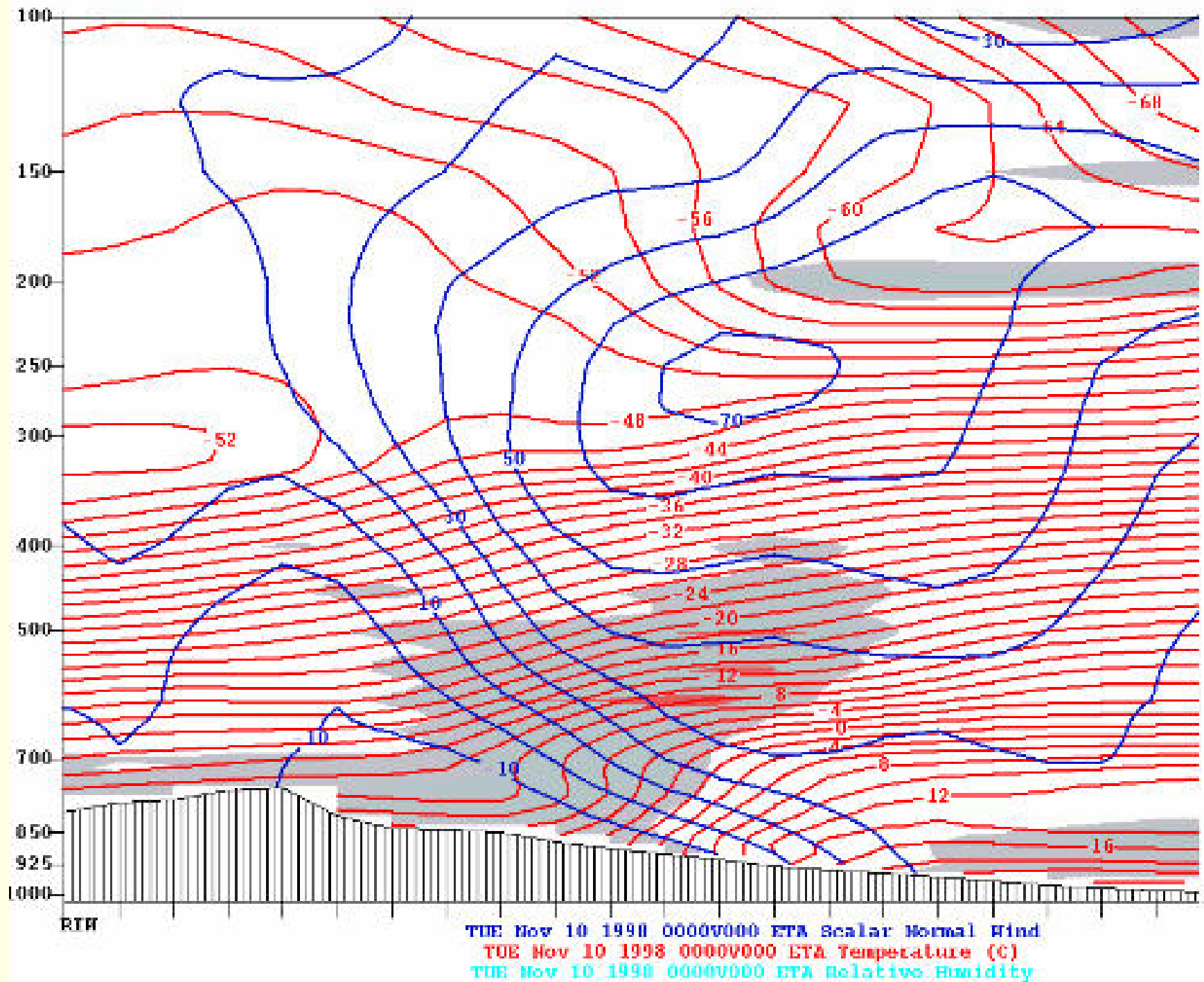
The front slopes backward toward the cold air, with increasing height. The front becomes less clearly defined at levels above 850 hPa.

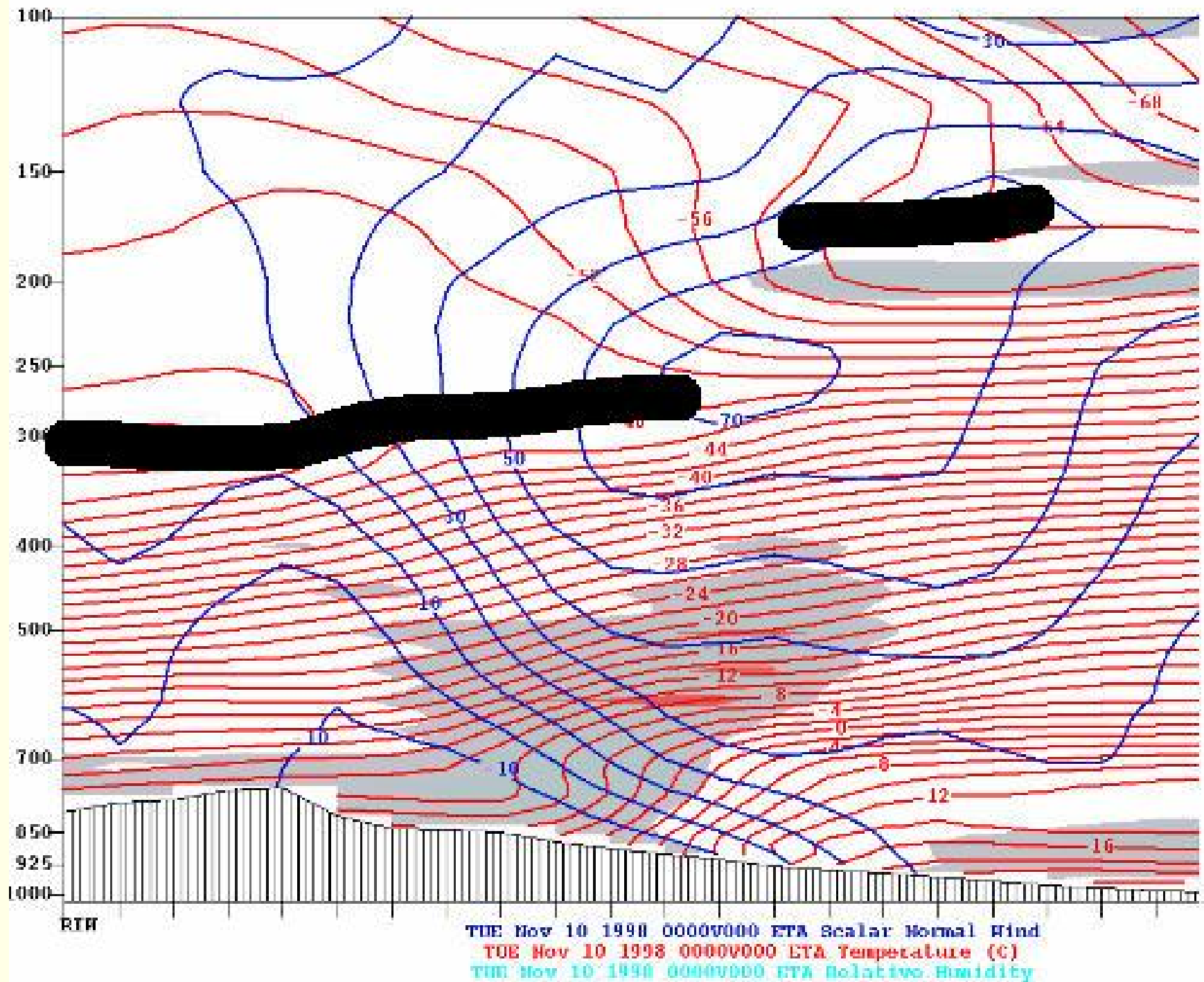
The jet stream passes through the section at the 250-hPa level, directly above the frontal zone.

The wind speed in the core of the jet stream is slightly in excess of 70 m/s.

The tropopause is clearly evident as a discontinuity in the vertical spacing of the isotherms: in the troposphere the isotherms are closely spaced in the vertical, indicative of strong lapse rates, while in the stratosphere, they are widely spaced, indicative of close-to-isothermal lapse rates.

The tropopause is low and relatively warm on the cyclonic (left) side of the jet stream and high and on the anticyclonic (right) side.





Alternatively, one can view the tropopause as being depressed over the cold, subsiding air mass and elevated over the warm air mass as a consequence of the **thermally direct circulations** in this rapidly developing baroclinic wave.

Alternatively, one can view the tropopause as being depressed over the cold, subsiding air mass and elevated over the warm air mass as a consequence of the **thermally direct circulations** in this rapidly developing baroclinic wave.

If one were to fly along the section at the jet stream (250-hPa) level, passing from the warm side to the cold side of the lower tropospheric frontal zone, one would cross from the upper troposphere to the lower stratosphere while crossing the jet stream.

Alternatively, one can view the tropopause as being depressed over the cold, subsiding air mass and elevated over the warm air mass as a consequence of the **thermally direct circulations** in this rapidly developing baroclinic wave.

If one were to fly along the section at the jet stream (250-hPa) level, passing from the warm side to the cold side of the lower tropospheric frontal zone, one would cross from the upper troposphere to the lower stratosphere while crossing the jet stream.

Entry into the stratosphere would be marked by a sharp decrease in relative humidity and an increase in the mixing ratio of ozone.

Alternatively, one can view the tropopause as being depressed over the cold, subsiding air mass and elevated over the warm air mass as a consequence of the **thermally direct circulations** in this rapidly developing baroclinic wave.

If one were to fly along the section at the jet stream (250-hPa) level, passing from the warm side to the cold side of the lower tropospheric frontal zone, one would cross from the upper troposphere to the lower stratosphere while crossing the jet stream.

Entry into the stratosphere would be marked by a sharp decrease in relative humidity and an increase in the mixing ratio of ozone.

One would also observe a marked increase in the **isentropic potential vorticity** of the ambient air: a consequence of the increase in static stability $-\partial\theta/\partial p$ in combination with a transition from weak anticyclonic relative vorticity ζ on the equatorward flank of the jet stream to quite strong cyclonic relative vorticity on the poleward flank.

IPV

Another variable frequently plotted in vertical cross sections is isentropic potential vorticity

$$\text{IPV} = -g(\zeta_{\theta} + f) \frac{\partial \theta}{\partial p}$$

a conservative tracer that serves as a marker for **intrusions of stratospheric air** into the troposphere in the vicinity of the jet stream.

IPV

Another variable frequently plotted in vertical cross sections is isentropic potential vorticity

$$\text{IPV} = -g(\zeta_{\theta} + f) \frac{\partial \theta}{\partial p}$$

a conservative tracer that serves as a marker for **intrusions of stratospheric air** into the troposphere in the vicinity of the jet stream.

Air that has been in the stratosphere for an appreciable time acquires high values of static stability $-\partial\theta/\partial p$ by virtue of the vertical gradient of diabatic heating at those levels.

IPV

Another variable frequently plotted in vertical cross sections is isentropic potential vorticity

$$\text{IPV} = -g(\zeta_{\theta} + f) \frac{\partial \theta}{\partial p}$$

a conservative tracer that serves as a marker for **intrusions of stratospheric air** into the troposphere in the vicinity of the jet stream.

Air that has been in the stratosphere for an appreciable time acquires high values of static stability $-\partial\theta/\partial p$ by virtue of the vertical gradient of diabatic heating at those levels.

When a layer of stratospheric air is drawn downward into the troposphere, columns are stretched in the vertical, pulling the potential temperature surfaces apart and thereby causing the static stability to decrease.

IPV

Another variable frequently plotted in vertical cross sections is isentropic potential vorticity

$$\text{IPV} = -g(\zeta_{\theta} + f) \frac{\partial \theta}{\partial p}$$

a conservative tracer that serves as a marker for **intrusions of stratospheric air** into the troposphere in the vicinity of the jet stream.

Air that has been in the stratosphere for an appreciable time acquires high values of static stability $-\partial\theta/\partial p$ by virtue of the vertical gradient of diabatic heating at those levels.

When a layer of stratospheric air is drawn downward into the troposphere, columns are stretched in the vertical, pulling the potential temperature surfaces apart and thereby causing the static stability to decrease.

Conservation of potential vorticity requires that the vorticity of the air become more cyclonic as it is stretched.

Second vertical cross-section

We now examine a vertical cross section normal the frontal zone twelve hours later, at 12 UTC November 10, 1998.

Second vertical cross-section

We now examine a vertical cross section normal the frontal zone twelve hours later, at 12 UTC November 10, 1998.

In this section the **red contours are isentropes** (rather than isotherms) and high values of isentropic potential vorticity, indicative of stratospheric air, are indicated by shading.

Second vertical cross-section

We now examine a vertical cross section normal the frontal zone twelve hours later, at 12 UTC November 10, 1998.

In this section the **red contours are isentropes** (rather than isotherms) and high values of isentropic potential vorticity, indicative of stratospheric air, are indicated by shading.

The jet stream is substantially stronger in this section than in the previous one, with peak wind speeds **in excess of 100 m/s**.

Second vertical cross-section

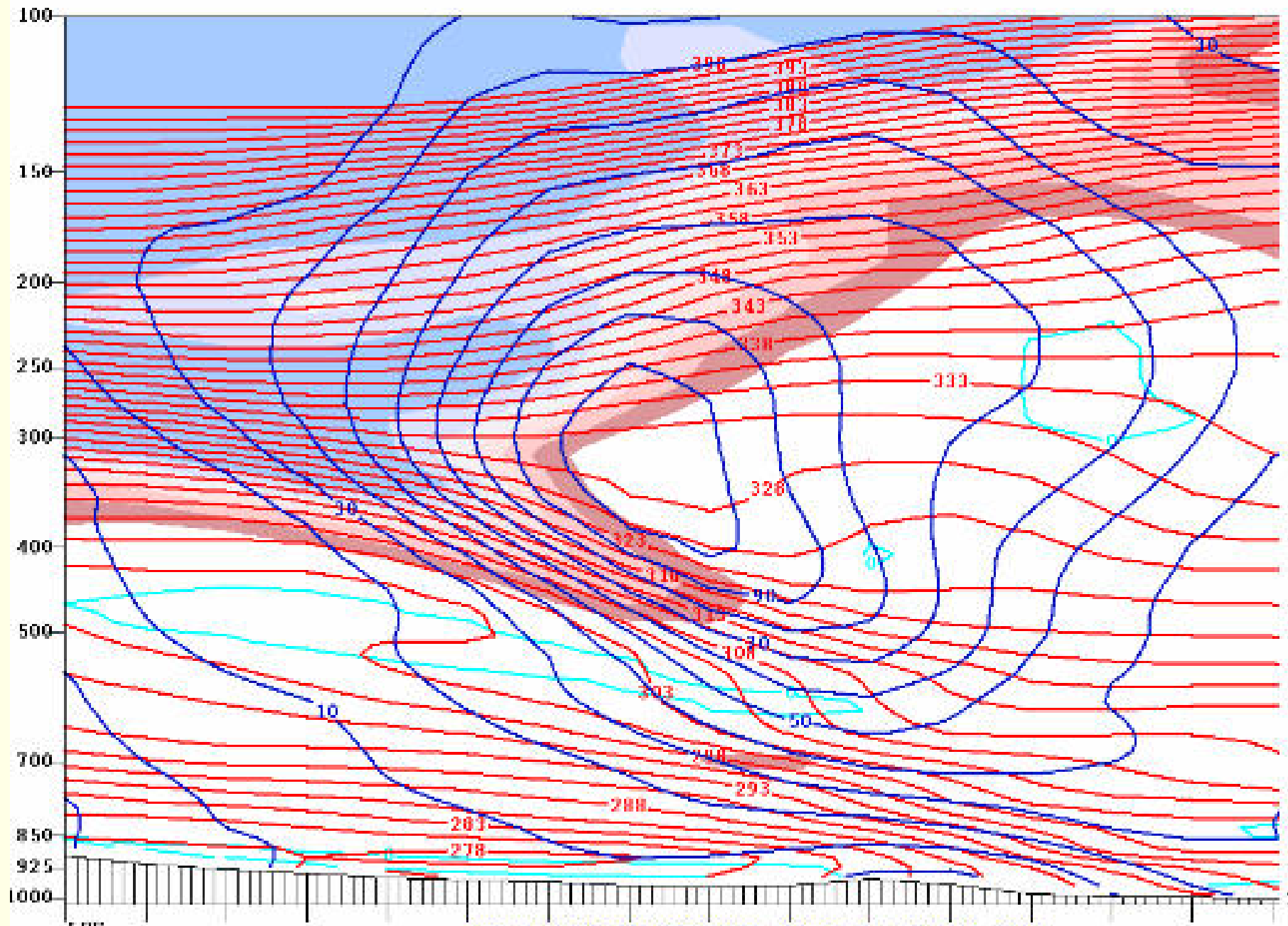
We now examine a vertical cross section normal the frontal zone twelve hours later, at 12 UTC November 10, 1998.

In this section the **red contours are isentropes** (rather than isotherms) and high values of isentropic potential vorticity, indicative of stratospheric air, are indicated by shading.

The jet stream is substantially stronger in this section than in the previous one, with peak wind speeds **in excess of 100 m/s**.

Immediately beneath the jet stream is a layer characterized by very strong vertical wind shear.

Consistent with the thermal wind equation, the horizontal gradient of temperature in this layer is also quite strong, with colder air to the left.



TUE Nov 10 1998 1200V000 ETA Scalar Normal Wind
 TUE Nov 10 1998 1200V000 ETA Potential Temperature
 TUE Nov 10 1998 1200V000 ETA Potential Vorticity

The air within this upper level frontal zone exhibits strong cyclonic relative vorticity by virtue of its cyclonic shear $\partial V_n / \partial s$ and it is also characterized by strong static stability, as evidenced by the tight vertical spacing of the isentropes.

The air within this upper level frontal zone exhibits strong cyclonic relative vorticity by virtue of its cyclonic shear $\partial V_n \partial s$ and it is also characterized by strong static stability, as evidenced by the tight vertical spacing of the isentropes.

It follows that the **isentropic potential vorticity** (IPV) of the air within this upper level frontal zone is **much higher** than that of typical air parcels at this level and the air within the core of the jet stream.

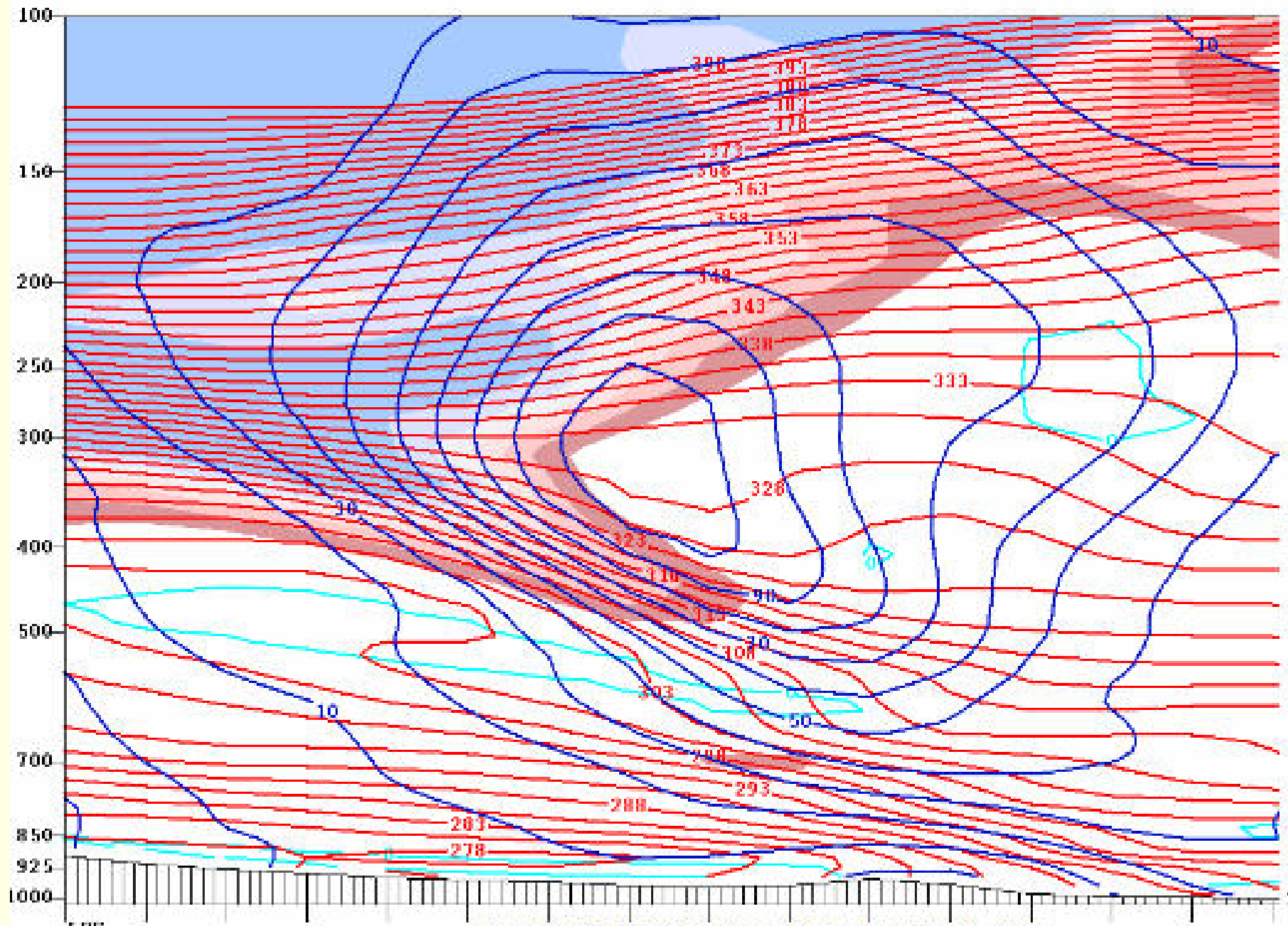
Accordingly, the IPV contours are folded backwards beneath the jet stream so as to include the upper tropospheric frontal zone within the region of high IPV.

The air within this upper level frontal zone exhibits strong cyclonic relative vorticity by virtue of its cyclonic shear $\partial V_n \partial s$ and it is also characterized by strong static stability, as evidenced by the tight vertical spacing of the isentropes.

It follows that the **isentropic potential vorticity** (IPV) of the air within this upper level frontal zone is **much higher** than that of typical air parcels at this level and the air within the core of the jet stream.

Accordingly, the IPV contours are folded backwards beneath the jet stream so as to include the upper tropospheric frontal zone within the region of high IPV.

Since the IPV contours define the boundary between tropospheric air and stratospheric air, it follows that the air within the frontal zone is of recent stratospheric origin.



TUE Nov 10 1998 1200V000 ETA Scalar Normal Wind
 TUE Nov 10 1998 1200V000 ETA Potential Temperature
 TUE Nov 10 1998 1200V000 ETA Potential Vorticity

Caption: Vertical cross-section of wind and potential temperature for 12 UTC November 10, 1998. Potential temperature is indicated by red contours and isotachs of geostrophic wind speed normal to the section, with positive values defined as southwesterly winds directed into the section, are plotted in blue. Isentropic potential vorticity in units of $10^{-6}\text{K m}^2 \text{s}^{-1}\text{kg}^{-1}$ (i.e., PVU) is indicated by shading.

★ ★ ★

Caption: Vertical cross-section of wind and potential temperature for 12 UTC November 10, 1998. Potential temperature is indicated by red contours and isotachs of geostrophic wind speed normal to the section, with positive values defined as southwesterly winds directed into the section, are plotted in blue. Isentropic potential vorticity in units of $10^{-6}\text{K m}^2 \text{s}^{-1}\text{kg}^{-1}$ (i.e., PVU) is indicated by shading.

★ ★ ★

The isentropic potential vorticity is plotted in PV units, that is $10^{-6}\text{K m}^2 \text{s}^{-1}\text{kg}^{-1}$, indicated by shading.

Caption: Vertical cross-section of wind and potential temperature for 12 UTC November 10, 1998. Potential temperature is indicated by red contours and isotachs of geostrophic wind speed normal to the section, with positive values defined as southwesterly winds directed into the section, are plotted in blue. Isentropic potential vorticity in units of $10^{-6}\text{K m}^2 \text{s}^{-1}\text{kg}^{-1}$ (i.e., PVU) is indicated by shading.

★ ★ ★

The isentropic potential vorticity is plotted in PV units, that is $10^{-6}\text{K m}^2 \text{s}^{-1}\text{kg}^{-1}$, indicated by shading.

When IPV is expressed in these units, the $\text{IPV} = 2.0$ surface usually conforms quite closely to the tropopause, with higher values above and lower values below.

Caption: Vertical cross-section of wind and potential temperature for 12 UTC November 10, 1998. Potential temperature is indicated by red contours and isotachs of geostrophic wind speed normal to the section, with positive values defined as southwesterly winds directed into the section, are plotted in blue. Isentropic potential vorticity in units of $10^{-6}\text{K m}^2 \text{s}^{-1}\text{kg}^{-1}$ (i.e., PVU) is indicated by shading.

★ ★ ★

The isentropic potential vorticity is plotted in PV units, that is $10^{-6}\text{K m}^2 \text{s}^{-1}\text{kg}^{-1}$, indicated by shading.

When IPV is expressed in these units, the $\text{IPV} = 2.0$ surface usually conforms quite closely to the tropopause, with higher values above and lower values below.

As we saw, the air within the frontal zone is of recent stratospheric origin. Such upper level frontal zones and their associated tropopause folds are the expressions of **extrusions of stratospheric air**, with high concentrations of ozone and other stratospheric tracers, into the upper troposphere.

Sometimes **tropopause folding** is a reversible process in which the high IPV air within the fold is eventually drawn back into the stratosphere.

At other times, the process is irreversible: the extruded stratospheric air becomes incorporated into the troposphere, where it eventually loses its distinctively high IPV.



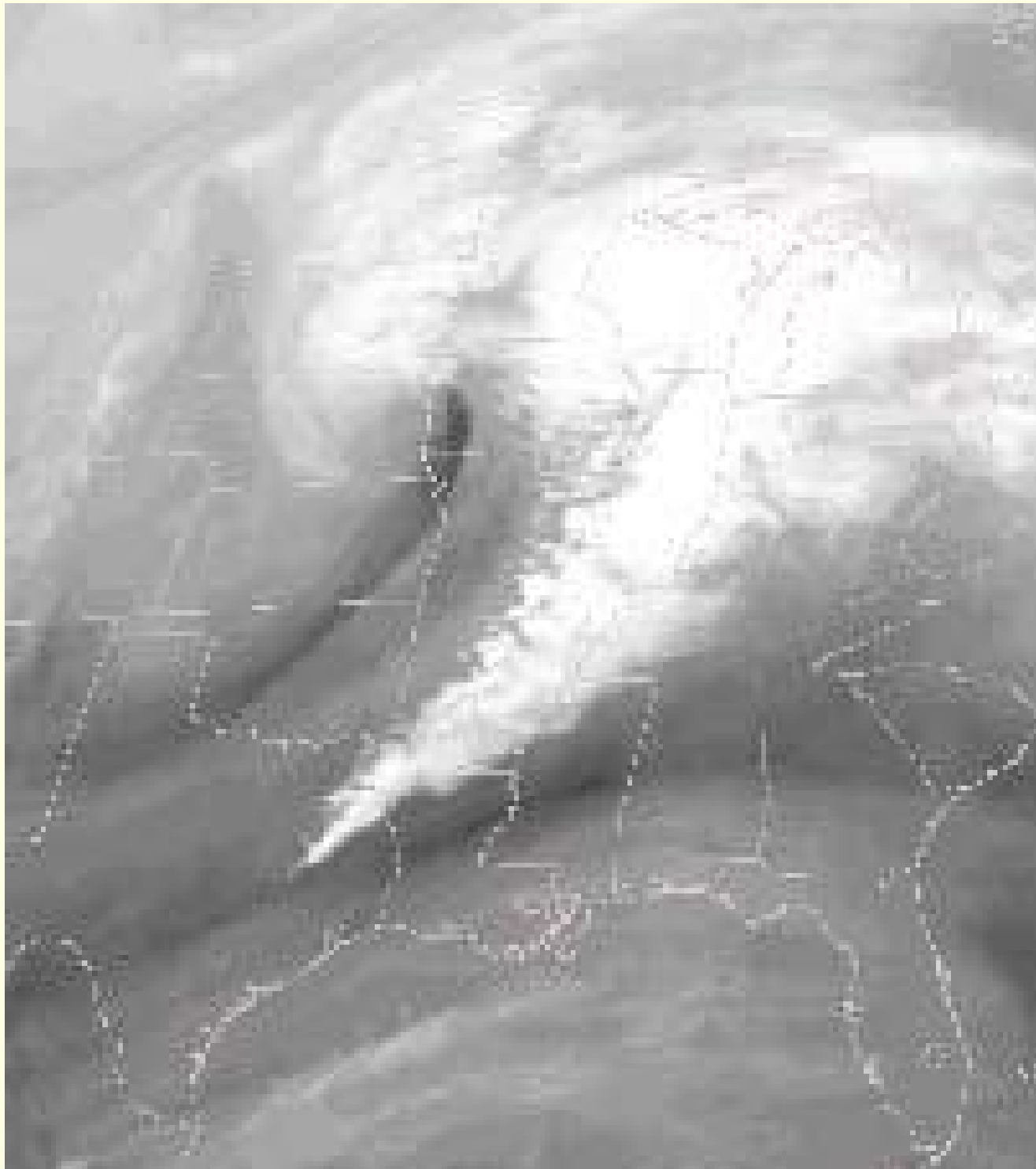
Sometimes **tropopause folding** is a reversible process in which the high IPV air within the fold is eventually drawn back into the stratosphere.

At other times, the process is irreversible: the extruded stratospheric air becomes incorporated into the troposphere, where it eventually loses its distinctively high IPV.

★ ★ ★

With the development of the cyclone, the stratospheric air was drawn downward and northeastward over the cold frontal zone, becoming an integral part of the **dry slot** in the water vapour satellite imagery.

The resulting injection of air with high IPV into the environment of the cyclone contributed to the **remarkable intensification** of this system during the later stages of its development.



WV image
09 UCT,
10 Nov., 1998.

Development processes

Baroclinic instability, in its pure form, is a **bottom up** process, involving the advection of the lower tropospheric meridional temperature gradient by the low level wind field.

Development processes

Baroclinic instability, in its pure form, is a **bottom up** process, involving the advection of the lower tropospheric meridional temperature gradient by the low level wind field.

In idealized numerical simulations, baroclinic waves reach their peak amplitude first in the *lower troposphere* and a day or so later at the jet stream level.

Development processes

Baroclinic instability, in its pure form, is a **bottom up** process, involving the advection of the lower tropospheric meridional temperature gradient by the low level wind field.

In idealized numerical simulations, baroclinic waves reach their peak amplitude first in the *lower troposphere* and a day or so later at the jet stream level.

In the real atmosphere, the location and timing of extra-tropical cyclone development (cyclogenesis) is influenced, and in some cases even dominated by dynamical processes in the upper troposphere.

Development processes

Baroclinic instability, in its pure form, is a **bottom up** process, involving the advection of the lower tropospheric meridional temperature gradient by the low level wind field.

In idealized numerical simulations, baroclinic waves reach their peak amplitude first in the *lower troposphere* and a day or so later at the jet stream level.

In the real atmosphere, the location and timing of extra-tropical cyclone development (cyclogenesis) is influenced, and in some cases even dominated by dynamical processes in the upper troposphere.

To generate a cyclone as intense as the one examined in this section, conditions in the upper and lower troposphere *must both be favourable*.

The region of cyclonic vorticity advection downstream of and on the cyclonic (i.e., poleward) side of a strong westerly jet is a favoured site for cyclogenesis, especially if it passes over a region of strong low-level baroclinicity.

The region of cyclonic vorticity advection downstream of and on the cyclonic (i.e., poleward) side of a strong westerly jet is a favoured site for cyclogenesis, especially if it passes over a region of strong low-level baroclinicity.

Extrusions of stratospheric air, with its high potential vorticity, into upper level frontal zones can increase the rate of intensification of the cyclonic circulation.

Another process that determines the sites most favourable for cyclogenesis is the eastward **dispersion of Rossby waves** at the jet stream level:

New baroclinic waves develop downstream of the existing ones, while the mature waves die out at the upstream end of the wavetrain.

Another process that determines the sites most favourable for cyclogenesis is the eastward **dispersion of Rossby waves** at the jet stream level:

New baroclinic waves develop downstream of the existing ones, while the mature waves die out at the upstream end of the wavetrain.

The relevance of this downstream development process is illustrated by the time-latitude plot of the meridional wind component at the jet stream (250-hPa) level for November 1998.

Time-latitude section of 250-hPa meridional wind averaged from 30° to 60°N for November 1998. N/A

Another process that determines the sites most favourable for cyclogenesis is the eastward **dispersion of Rossby waves** at the jet stream level:

New baroclinic waves develop downstream of the existing ones, while the mature waves die out at the upstream end of the wavetrain.

The relevance of this downstream development process is illustrated by the time-latitude plot of the meridional wind component at the jet stream (250-hPa) level for November 1998.

Time-latitude section of 250-hPa meridional wind averaged from 30° to 60°N for November 1998. N/A

From this section it is evident that the cyclone that developed over the central United States ($\sim 90^\circ\text{W}$) November 10 was part of a **well-defined wave packet** that propagated eastward with a group velocity of around 20 m/s, roughly twice the rate of propagation of the individual waves within the packet.

Final Word of Caution

We end our discussion on the structure and life cycle of extratropical cyclones with a disclaimer:

No single case study can do justice to the diversity and complexity of the structure and evolution of extratropical weather systems. The structure of fronts and rain bands varies widely from case to case and the ideal textbook example is rarely, if ever observed.

Final Word of Caution

We end our discussion on the structure and life cycle of extratropical cyclones with a disclaimer:

No single case study can do justice to the diversity and complexity of the structure and evolution of extratropical weather systems. The structure of fronts and rain bands varies widely from case to case and the ideal textbook example is rarely, if ever observed.

Even in the nearly perfect storm examined in this section, the warm front was difficult to follow and the presence of a secondary cold front complicated the interpretation of the surface maps and many of the time series.

Final Word of Caution

We end our discussion on the structure and life cycle of extratropical cyclones with a disclaimer:

No single case study can do justice to the diversity and complexity of the structure and evolution of extratropical weather systems. The structure of fronts and rain bands varies widely from case to case and the ideal textbook example is rarely, if ever observed.

Even in the nearly perfect storm examined in this section, the warm front was difficult to follow and the presence of a secondary cold front complicated the interpretation of the surface maps and many of the time series.

Hence, the example should be interpreted not as a comprehensive description of extratropical cyclones, but as an in-depth example designed to illustrate these remarkable atmospheric systems.